78N29068

NASA Technical Memorandum 78492

AVRADCOM Technical Report 78-15 (AM)

Closed-Form Equations for the Lift, Drag, and Pitching-Moment Coefficients of Airfoil Sections in Subsonic Flow

Roger L. Smith, Aeromechanics Laboratory
AVRADCOM Research and Technology Laboratories
Ames Research Center, Moffett Field, California

National Aeronautics and
Space Administration

Ames Research Center
Moffett Field, California 94035

United States Army
Aviation Research and
Development Command
St. Louis, Missouri 63166

CLOSED-FORM EQUATIONS FOR THE LIFT, DRAG, AND PITCHING-MOMENT COEFFICIENTS OF AIRFOIL SECTIONS IN SUBSONIC FLOW

Roger L. Smith

Ames Research Center
and
Aeromechanics Laboratory, AVRADCOM Research and Technology Laboratories

SUMMARY

Closed-form equations for the lift, drag, and pitching-moment coefficients of two-dimensional airfoil sections in steady subsonic flow are obtained from published theoretical and experimental results. A turbulent boundary layer is assumed to exist on the airfoil surfaces. The effects of section angle of attack, Mach number, Reynolds number, and the specific airfoil type are considered. The equations are applicable through an angle-of-attack range of -180° to +180°; however, above about ±20°, the section characteristics are assumed to be functions only of angle of attack. A computer program is presented which evaluates the equations for a range of Mach numbers and angles of attack. Calculated results for the NACA 23012 airfoil section are compared with experimental data.

NOMENCLATURE

c	airfoil chord, m
c_d	drag coefficient
c_F	friction drag coefficient
c_f	mean skin friction coefficient
c_ℓ	lift coefficient
$c_{\ell_{max}}$	maximum lift coefficient (first lift-curve peak)
c_m	pitching-moment coefficient about quarter-chord
c_{m_0}	pitching-moment coefficient at $\alpha = 0$
c_s	pressure (form) drag coefficient
K	correlation parameter for airfoil drag due to lift

L	airfoil section perimeter, m
M	Mach number
M_{DD}	drag divergence Mach number
M_{MD}	moment divergence Mach number
M_1	Mach number at which trend of increasing lift-curve slope with increasing M reverses; also, highest Mach number for which c_{ℓ_α} is invariant with M
R_N	Reynolds number
R_{N_1}	Reynolds number based on free-stream velocity
S_A	mean value of airfoil pressure coefficient
t	airfoil section maximum thickness, m
α	airfoil section angle of attack, deg
α_c	cutoff α, above which the slope of c_d with M is assumed to be constant, deg
$\alpha_{P_{DD}}$	α corresponding to highest value of M_{DD}, deg
$\alpha_{P_{MD}}$	α corresponding to highest value of M_{MD}, deg
α_R	reference angle about which dc_d/dM vs α curve is assumed to be a mirror image, deg
α_{stall}	airfoil section stall angle, approximated as $\frac{c_{\ell_{max}}}{dc_\ell/d\alpha} + \alpha_0$, deg
α_0	angle of attack for zero lift, deg
γ	ratio of specific heats

INTRODUCTION

Piloted simulation of helicopters or other rotorcraft in real time is paced by the speed of solution of the rotor dynamic equations of motion. One method of increasing computation speed is the use of a hybrid (analog plus digital) computer, with all rotor calculations being accomplished in the analog computer. Unfortunately, this may preclude the normal practice of providing rotor blade airfoil section characteristics in tabular form, since the time required for the very large number of table lookups may negate the expected speed advantage. Therefore, it was determined to derive closed-form equations for the lift, drag, and pitching moment of airfoil sections which

would exhibit, insofar as possible and practical, the effects of angle of attack, Mach number, Reynolds number, and the specific section type. Published airfoil data were used to establish the form of equations which both reflect general trends and accommodate specific section type characteristics where possible. The coefficients of the equations must be obtained from experimental data for the particular airfoil of interest, but the data requirements are not as extensive as for construction of airfoil data tables typically used in helicopter rotor analysis programs.

The equations presented herein are equally applicable to fixed-wing problems, and should be useful in any case where it is either impractical or impossible to use an airfoil section data table. Conversely, if a particular data table is desired but not available, the equations provide a means of generating the table (with angle of attack and Mach number as parameters) from limited input data.

ASSUMPTIONS AND LIMITATIONS

The equations presented herein were derived from experimental airfoil section data obtained under conditions of two-dimensional, steady-state flow. The airfoil surface condition is assumed to be representative of in-service conditions; that is, smooth, but with a turbulent boundary layer over essentially the entire airfoil. Considering the combined effects of manufacturing defects, service wear, environmental deposits, high Reynolds number and free-stream turbulence, it is reasonable, if slightly conservative, to assume a fully turbulent boundary layer for all full-scale rotors and wings for which no special laminar flow apparatus is provided (ref. 1). The assumption of a turbulent boundary layer establishes the form of the incompressible drag coefficient (appendix B).

The subject equations are applicable only for flight conditions in which the free-stream Mach number is less than one. The Reynolds number, based on section chord, is assumed to be greater than 1×10^6. Certain experimental data for the particular airfoil type under consideration must be available. Two examples of such data are: (1) moment coefficient at low Mach number and zero angle of attack; and (2) at least two values of drag divergence Mach number as a function of section angle of attack. All such requirements are presented in a subsequent section.

Equations are provided in this report for section lift, drag, and pitching moment coefficient through an angle of attack range of ±180°. However, above about ±20°, these coefficients are functions only of angle of attack, and are independent of Mach number, Reynolds number, and the airfoil type. This simplification is a consequence of the very small amount of experimental data available at high angle of attack.

It is assumed that the equations presented in this report will be applied only to airfoils whose characteristics follow the same general trends as the experimental data used to derive the equations (see the appendixes). For

example, the drag divergence Mach number should be at least approximately linear with section angle of attack.

AIRFOIL SECTION FORCE AND MOMENT EQUATIONS

Equations for the lift, drag, and pitching moment of airfoil sections through ±180° angle of attack, derived in appendixes A, B, and C, respectively, are presented below. The equations are principally empirical in nature, and in the low angle of attack range require as input experimental data for the particular airfoil type. These requirements are discussed in a subsequent section. Assumptions and limitations are given in the preceding section. To facilitate reference to the appropriate section of the appendixes, equation numbers from the appendixes are retained here.

Lift Coefficient

Small angle of attack ($\alpha \le \alpha_{stall}$)-

$$c_\ell = \frac{dc_\ell}{d\alpha}(\alpha - \alpha_0), \qquad |\alpha| \le |\alpha_{stall}| \tag{A1}$$

$$\left(\frac{dc_\ell}{d\alpha}\right) = \left(\frac{dc_\ell}{d\alpha}\right)_{inc}\left\{\mu + \frac{t/c}{1 + t/c}\left[\mu(\mu - 1) + 0.6(\mu^2 - 1)\right]\right\} \tag{A2}$$

where

$$\mu = \frac{1}{\sqrt{1 - M^2}}$$

If $M > M_1$, use

$$\frac{dc_\ell}{d\alpha} = \left(\frac{dc_\ell}{d\alpha}\right)_{inc}\left\{\mu + \frac{t/c}{1 + t/c}\left[\mu(\mu - 1) + 0.6(\mu^2 - 1)\right]\right\} - (0.45)(M - M_1) \tag{A3}$$

in lieu of equation (A2), but set $dc_\ell/d\alpha = 0.05$ as a lower limit.

$$\alpha_0 = (\alpha_0)_1, \qquad 0 \le M \le M_1 \tag{A4}$$

$$\alpha_0 = (\alpha_0)_1 - \frac{(\alpha_0)_1 - (\alpha_0)_2}{M_1 - M_2}(M_1 - M), \qquad M > M_1 \tag{A5}$$

$$c_{\ell_{max}} = C_1 + C_2M + C_3M^2 + C_4M^3 + C_5M^4 + (C_6 + C_7M^{C_8})\sin(C_9 + C_{10}M) \tag{A6}$$

For negative angle of attack, the form of $c_{\ell_{max}}$ is assumed to be given by equation (A6). The sign of $c_{\ell_{max}}$ will be negative, and for cambered sections the constant term C_1 will have a different magnitude also.

Large angle of attack- For positive angles of attack,

$$c_\ell = 0.813 + \frac{c_{\ell_{max}} - 0.813}{22 - \alpha_{stall}} (22 - \alpha) , \qquad \alpha_{stall} < \alpha < 22^\circ , \tag{A16}$$

where

$$\alpha_{stall} = \frac{c_{\ell_{max}}}{dc_\ell/d\alpha} + \alpha_0 \tag{A17}$$

$$c_\ell = 1.1 - 1.78[0.01745(\alpha) - 0.7853]^2 , \qquad 22^\circ \le \alpha < 90^\circ \tag{A8}$$

$$c_\ell = -1.1 + 1.78[0.01745(\alpha) - 2.356]^2 , \qquad 90^\circ \le \alpha < 160^\circ \tag{A9}$$

$$c_\ell = -0.763 , \qquad 160^\circ \le \alpha < 172.5^\circ \tag{A10}$$

$$c_\ell = -5.82[\pi - 0.01745(\alpha)] , \qquad 172.5^\circ \le \alpha \le 180^\circ \tag{A11}$$

For negative angles of attack:

$$c_\ell = -0.813 + \frac{\left(c_{\ell_{max}}\right)_{-\alpha} + 0.813}{22 + \alpha_{neg\ stall}} (22 + \alpha) , \qquad -22^\circ < \alpha < \alpha_{neg\ stall} \tag{A18}$$

where

$$\alpha_{neg\ stall} = \frac{\left(c_{\ell_{max}}\right)_{-\alpha}}{dc_\ell/d\alpha} + \alpha_0 \tag{A19}$$

$$c_\ell = -1.1 + 1.78[0.01745|\alpha| - 0.7853]^2 , \qquad -90^\circ < \alpha \le -22^\circ \tag{A12}$$

$$c_\ell = 1.1 - 1.78[0.01745|\alpha| - 2.356]^2 , \qquad -160^\circ < \alpha \le -90^\circ \tag{A13}$$

$$c_\ell = 0.763 , \qquad -172.5^\circ < \alpha \le -160^\circ \tag{A14}$$

$$c_\ell = 5.82[\pi - 0.01745|\alpha|] , \qquad -180^\circ \le \alpha \le -172.5^\circ \tag{A15}$$

Drag Coefficient

Small angle of attack ($|\alpha| \leq \alpha_{stall}$)-

$$M_{DD} = A + b\alpha , \qquad \alpha \geq \alpha_{P_{DD}} \tag{B6}$$

$$M_{DD} = C + D\alpha , \qquad \alpha < \alpha_{P_{DD}} \tag{B7}$$

$$M_{DD} \geq 0.3 \quad \text{for any } \alpha$$

For Mach number less than the drag divergence Mach number,

$$c_d = (c_d)_{M=0} , \qquad M \leq M_{DD} , \qquad \alpha \leq \alpha_{stall} \tag{B1}$$

$$(c_d)_{M=0} = (c_f)\left[S_A \frac{L}{c}\left(1 + \frac{c_s}{c_F}\right) + \frac{K(0.01745\alpha)^2}{(c_f)_{R_N=6\times10^6}}\right] \tag{B3}$$

$$c_f = \frac{0.455}{\left(\log R_{N_{eff}}\right)^{2.58}} , \tag{B4}$$

$$R_{N_{eff}} = R_N \left(\frac{1}{2}\frac{L}{c}\right) S_A , \tag{B5}$$

For Mach number greater than the drag divergence Mach number:

$$c_d = (c_d)_{M=0} + \frac{dc_d}{dM}(M - M_{DD}) , \qquad M > M_{DD} , \qquad \alpha \leq \alpha_{stall} \tag{B2}$$

$$\frac{dc_d}{dM} = A + B\alpha + C\alpha^2 + D\alpha^3 , \qquad \alpha_R \leq \alpha \leq \alpha_c \tag{B8}$$

$$\frac{dc_d}{dM} = \left(\frac{dc_d}{dM}\right)_{\alpha=\alpha_c} , \qquad \alpha > \alpha_c \tag{B9}$$

For angles of attack less (more negative) than the reference angle α_R, substitute

$$\alpha' = |\alpha| + 2\alpha_R , \qquad \alpha < \alpha_R \tag{B10}$$

in equation (B8). Also the negative angle at which dc_d/dM becomes constant is

$$\alpha_c' = -\alpha_c + 2\alpha_R \tag{B11}$$

Large angle of attack-

$$c_d = 0.219 - \frac{0.219 - (c_d)_{\alpha_{stall}}}{15 - |\alpha_{stall}|}(15 - |\alpha|), \quad |\alpha_{stall}| \leq |\alpha| \leq 15^\circ \tag{B13}$$

where

$$\alpha_{stall} = \frac{c_{\ell_{max}}}{dc_\ell/d\alpha} + \alpha_0 \tag{B14}$$

$$c_d = 2.18(|\sin \alpha|)^{1.2}, \quad 15^\circ \leq |\alpha| \leq 180^\circ \tag{B12}$$

For negative angle of attack, $c_{\ell_{max}}$ in equation (B14) is replaced by $(c_{\ell_{max}})_{-\alpha}$.

Pitching Moment Coefficient

Small angle of attack ($|\alpha| \leq 20^\circ$)-

$$M_{MD} = A + B\alpha, \quad \alpha \leq \alpha_{P_{MD}} \tag{C2}$$

$$M_{MD} = C + D\alpha, \quad \alpha > \alpha_{P_{MD}} \tag{C3}$$

$$M_{MD} \geq 0.3 \quad \text{for any } \alpha$$

$$c_m = c_{m_0} + \frac{dc_m}{d\alpha}(\alpha), \quad M \leq M_{MD}, \quad |\alpha| \leq \alpha_{stall} \tag{C1}$$

$$c_m = -0.077 + \frac{(c_m)_{\alpha_{stall}} + 0.077}{20 - \alpha_{stall}}(20 - \alpha), \quad 20^\circ > \alpha > \alpha_{stall} \tag{C4}$$

$$c_m = (c_m)_{MD} - \frac{(c_m)_{MD} + 0.077}{0.95 - M_{MD}}(M - M_{MD}), \quad M > M_{MD} \tag{C5}$$

For negative angles of attack:

$$c_m = 0.077 - \frac{0.077 - (c_m)_{\alpha_{stall}}}{20 + \alpha_{stall}}(20 + \alpha), \quad 20^\circ > |\alpha| > |\alpha_{stall}| \tag{C6}$$

$$c_m = (c_m)_{MD} - \frac{(c_m)_{MD} - 0.077}{0.95 - M_{MD}}(M - M_{MD}), \quad M > M_{MD} \tag{C7}$$

where α_{stall} is negative.

Large angle of attack-

$$c_m = -0.00802\ (\alpha - 20) - 0.077\ , \qquad 20° \leq \alpha \leq 67° \tag{C8}$$

$$c_m = -0.619[\sin(0.0260\alpha - 1.26)]^{0.398}\ , \qquad 67° \leq \alpha \leq 162° \tag{C9}$$

$$c_m = -0.00838(\alpha - 162) - 0.320\ , \qquad 162° \leq \alpha \leq 170° \tag{C10}$$

$$c_m = 0.0387\ (\alpha - 170) - 0.387\ , \qquad 170° \leq \alpha \leq 180° \tag{C11}$$

For negative angles of attack:

$$c_m = 0.00802(|\alpha| - 20) + 0.077\ , \qquad -67° \leq \alpha \leq -20° \tag{C12}$$

$$c_m = 0.619[\sin(0.0260|\alpha| - 1.26)]^{0.398}\ , \qquad -162° \leq \alpha \leq -67° \tag{C13}$$

$$c_m = 0.00838(|\alpha| - 162) + 0.320\ , \qquad -170° \leq \alpha \leq -162° \tag{C14}$$

$$c_m = -0.0387(|\alpha| - 170) + 0.387\ , \qquad -180° \leq \alpha \leq -170° \tag{C15}$$

INPUT DATA REQUIREMENTS

The input data that are necessary for evaluation of the lift, drag, and pitching moment equations can be obtained from airfoil section test results. The specific input variables, and the equations in which they are used, are listed in table 1. (It should be noted that S_A, L/c, c_s/c_p, and K, which are used in the drag equations (B3) and (B5), can be obtained from figs. 7-10, appendix B, respectively, as functions of section thickness t/c.)

Minimum experimental data (for a particular airfoil) necessary to evaluate the inputs listed in table 1 are:

c_ℓ vs α for several M from zero to M_2

c_d vs M for several α

c_m vs M for several α

The effort required for data preparation will be reduced if the following curves are also available:

$c_{\ell_{max}}$ vs M

M_{DD} vs α

M_{MD} vs α

c_m vs α, for a low M

The c_ℓ vs α curves should extend to at least the stall angle. No test data past stall are required because the airfoil section characteristics at high angles of attack are assumed to be independent of section type. The appendixes provide a guide to the use of the above data in the preparation of input.

EXAMPLE CASE

The equations presented above were used to calculate lift, drag, and pitching moment coefficients for the NACA 23012 airfoil section. Input data were obtained from wind tunnel test results for the 23012 given in references 2-4, and are listed in table 2. The calculations were done by a digital computer program written to evaluate the equations over a range of Mach number and angle of attack. A FORTRAN listing of the program is presented in appendix D. Section coefficients were calculated through an angle of attack range of -180° to +180°, and through a Mach number range of 0.0 to 0.9. From these results, c_ℓ, c_d, and c_m at $M = 0.1$, for $\alpha = -20°$ to +180°, are plotted in figure 1.

Calculated and measured (ref. 2) section aerodynamic characteristics at low angle of attack for three Mach numbers, are compared in figure 2. Overall good agreement was realized, although some details of the 23012 behavior were not reproduced, since the equations are intended to be sufficiently general to represent most airfoil sections. No effort was made to tailor the inputs to improve the correlation. Experimental data for the 23012 at high angle of attack were not available. Figure 3 presents measured and calculated section coefficients as a function of Mach number. In this case, the experimental data are from reference 4. Again, generally good agreement was found.

CONCLUDING REMARKS

The airfoil section equations presented in this report were developed principally by fitting curves to a relatively limited set of experimental data. Some accuracy was sacrificed to obtain general applicability to a range of airfoil types. The utility of such equations can be judged only in the context of their intended use. If high accuracy is not required, these equations provide the ability to calculate airfoil section aerodynamic coefficients at any angle of attack, over a wide range of subsonic Mach numbers.

The principal application of the equations will be in fixed or rotary wing computations for which it is not practical to use graphical or tabulated section data, or for which a data table must be generated from limited input. The equations also provide a method for calculating section lift, drag, and pitching moment at very high angles of attack (i.e., $-180° \leq \alpha \leq 180°$). Experimental data of this type are available for very few airfoils. Another important application is in the prediction of section characteristics at high subsonic Mach numbers in cases where such data are incomplete.

APPENDIX A

DERIVATION OF LIFT COEFFICIENT EQUATIONS

SMALL ANGLE OF ATTACK

In the section angle of attack range $0 \leq |\alpha| \leq 22°$, effects of compressibility, Reynolds number, and the specific airfoil section of interest are considered. For angles of attack below the stall, the section lift curve is assumed to be linear:

$$c_\ell = \frac{dc_\ell}{d\alpha}(\alpha - \alpha_{c_\ell=0}) , \qquad |\alpha| \leq |\alpha|_{stall} \tag{A1}$$

Lift-Curve Slope

Mach number and thickness effects- Kaplan's rule (ref. 3) is used to represent the effects of compressibility and airfoil section thickness on lift curve slope:

$$\left(\frac{dc_\ell}{d\alpha}\right)_{comp} = \left(\frac{dc_\ell}{d\alpha}\right)_{inc}\left\{\mu + \frac{t/c}{1 + t/c}\left[\mu(\mu - 1) + \frac{1}{4}(\gamma + 1)(\mu^2 - 1)^2\right]\right\}$$

where

$$\mu = \frac{1}{\sqrt{1 - M^2}}$$

$\frac{t}{c}$ = section thickness to chord ratio

γ = 1.4 for air

so that

$$\left(\frac{dc_\ell}{d\alpha}\right)_{comp} = \left(\frac{dc_\ell}{d\alpha}\right)_{inc}\left\{\mu + \frac{t/c}{1 + t/c}\left[\mu(\mu - 1) + 0.6(\mu^2 - 1)^2\right]\right\} \tag{A2}$$

The utility of this relation was investigated by comparing calculated and measured (ref. 2) lift-curve slopes for several airfoils over a range of Mach numbers, as shown in table 3. Lift-curve slope at M above 0.3 was obtained from the measured value at M = 0.3 and the ratio

$$\frac{(dc_\ell/d\alpha)_{M>0.3}}{(dc_\ell/d\alpha)_{M=0.3}} ,$$

calculated with equation (A2). The difference between the calculated and the measured lift-curve slope was 10% or less except for one Mach number for one airfoil.

For the airfoils considered in table 3, and other airfoils presented in reference 2, the trend of increasing lift-curve slope with Mach number reverses above approximately M = 0.8. However, there is no discernible pattern to the rate of decline. References 5 and 6 present "synthesized" airfoil section data (for the NACA 0012 and 0015, respectively) which do exhibit a smooth decline of lift-curve slope above the reversal. This smoothness is due to the manner in which the airfoil characteristics were derived: an iteration between successive assumption of airfoil data values and comparison of calculated with measured rotor performance. The average rate of decline of lift-curve slope for the two sets of section data is

$$\frac{(dc_\ell/d\alpha)_M}{} = -0.45 \text{ per deg}$$

Let M at which the trend of the lift-curve slope reverses be M_1. Then, for M above M_1, the lift-curve slope will be

$$\frac{dc_\ell}{d\alpha} = \left(\frac{dc_\ell}{d\alpha}\right)_{comp} - (0.45)(M - M_1), \text{ per deg}$$

$$\frac{dc_\ell}{d\alpha} = \left(\frac{dc_\ell}{d\alpha}\right)_{inc}\left\{ + \frac{t/c}{1 + t/c}\left[\mu(\quad - 1) + 0.6(\quad - 1)^2\right]\right\} - (0.45)(M - M_1) \tag{A3}$$

It is necessary to set a lower limit for equation (A3). Again, the data available (e.g., ref. 2) are not sufficiently regular to provide a trend. Therefore, the lift-curve slope for the highest Mach number presented was measured for several airfoils in reference 2. The average value is 0.05. Thus the lower limit of equation (A3) is assumed to be

$$\frac{dc_\ell}{d\alpha} \geq 0.05 \text{ per deg}$$

Reynolds number effects- Airfoil section lift-curve slope is a weak function of R_N up to 1×10^7 or 2×10^6, and is essentially independent of R_N for higher values (refs. 2 and 3). Therefore, for most uses, lift-curve slope can be assumed to be constant with R_N. The value of incompressible lift-curve slope used in equation (A3) should be selected with consideration for the likely R_N range to be encountered. This value is also a function of the specific airfoil section considered.

Angle of Zero Lift

Mach number effects- The variation of airfoil section angle of zero lift, α_0, is small with M and may be neglected, until M reaches a high subsonic

value. Then, for most airfoils, α_0 decreases in magnitude with further increases in M. Table 4 presents measured α_0 values for M above M_1, where M_1 is the highest M in the experimental data for which α_0 remains at a constant value. (The Mach number M_1 is also the Mach number at which the trend of increasing lift-curve slope with increasing M reverses.) The data in table 4 provide no consistent trend. For six of the sections, there is a strong decrease in the magnitude of α_0 with M, for M above M_1. However, for three of the sections, the decline of α_0 is slight, while for two other sections, the decline of α_0 is reversed as M continues to increase. Since a general expression for α_0 was desired, it was assumed that the variation of section angle of zero lift with M can be adequately represented by a straight line above M_1:

$$\alpha_0 = (\alpha_0)_1 , \qquad 0 \le M \le M_1 \tag{A4}$$

$$\alpha_0 = (\alpha_0)_1 - \frac{(\alpha_0)_1 - (\alpha_0)_2}{M_1 - M_2} (M_1 - M) , \qquad M > M_1 \tag{A5}$$

Mach number M_2 is some convenient $M > M_1$ for which α_0 can be determined from the experimental section data. Note that for symmetrical airfoil sections, $\alpha_0 = 0$ even for high Mach numbers. Thus, for symmetrical sections, $\alpha_0 = (\alpha_0)_1 = (\alpha_0)_2 = 0$.

Reynolds number effects- The angle of zero lift (low Mach number) of an airfoil section is determined by the camber. The extensive section data presented in reference 3 indicate that α_0 is not significantly affected by Reynolds number.

Maximum Lift Coefficient

Mach number effects- In the angle of attack range below the first lift peak, the variation of airfoil section maximum lift coefficient, $c_{\ell_{max}}$, with M may be categorized as: (1) throughout the range of interest, $c_{\ell_{max}}$ decreases with M, or (2) in part of the range, $c_{\ell_{max}}$ increases with M (but decreases otherwise). Experimental data for both types are shown by the solid curves in figure 4, and both can be fitted by polynomials of the form

$$c_{\ell_{max}} = C_1 + C_2M + C_3M^2 + C_4M^3 + C_5M^4 + (C_6 + C_7M^{C_8})\sin(C_9 + C_{10}M) \tag{A6}$$

Fits for two specific airfoil sections are shown by the dashed lines in figure 4. For the V23010 - 1.58 (type 1 above), only the first three terms of equation (A6) were required. However, for the VR-7 (type 2 above), all ten coefficients are nonzero. In both cases, the functions were obtained by use of a least-squares curve-fit program.

Reynolds number effects- Figure 5, from reference 2, presents the combined effects of M and R_N for two airfoil sections. It can be seen that the

effect of increasing R_N is to shift the complete $c_{\ell_{max}}$ vs M curve upwards, with the curves tending to collapse together above about $R_N = 3\times10^6$ in one case, and above about $R_N = 6\times10^6$ for the other. Therefore, the constant C_1 in equation (A6) above will be determined (from low M experimental data for the particular section) as a function of the expected R_N range.

Negative angle of attack- Experimental data for $c_{\ell_{max}}$ at negative angle of attack, as a function of M, are not available for most airfoil sections. It is assumed that the variation of $c_{\ell_{max}}$ with M at negative α has the same form as for positive α. The sign of $c_{\ell_{max}}$ is negative, of course, and for cambered sections the constant term C_1 in equation (A6) will have a different magnitude as well as a different sign. The C_1 term is obtained from the experimental lift curve at low M. If no data are available for negative $c_{\ell_{max}}$ even for low M, it can be estimated as

$$\left(c_{\ell_{max}}\right)_{-\alpha} = -\left[\left(c_{\ell_{max}}\right)_{+\alpha} - 2(\Delta c_\ell)_{\alpha=0}\right] \tag{A7}$$

That is, for a cambered section, negative $c_{\ell_{max}}$ is lower in magnitude than the positive $c_{\ell_{max}}$ by an amount double the lift increment due to the camber. The accuracy of this estimate was evaluated by comparing it with measured values for several airfoil sections, as presented in table 5. The error is less than 10% in six of the seven cases studied.

LARGE ANGLE OF ATTACK

Very little experimental section lift coefficient data for angle of attack more than a few degrees above the stall angle are available. Section lift coefficients through 180° for the NACA 0012 and the NACA 63A012 are presented in figure 6. A curve fit of these data in four segments is given by

$$c_\ell = 1.1 - 1.78[0.01745(\alpha) - 0.7853]^2 , \quad 22° \le \alpha \le 90° \tag{A8}$$

$$c_\ell = -1.1 + 1.78[0.01745(\alpha) - 2.356]^2 , \quad 90° \le \alpha \le 160° \tag{A9}$$

$$c_\ell = -0.763 , \quad 160° \le \alpha \le 172.5° \tag{A10}$$

$$c_\ell = -5.82[\pi - 0.01745(\alpha)] , \quad 172.5° \le \alpha \le 180° \tag{A11}$$

Equations (A8) through (A11) are taken from reference 7, except that (A8) is begun at $\alpha = 22°$ rather than 16° since this yields better agreement with the experimental data in figure 6.

It is assumed that airfoil section lift coefficient at large angles of attack is an odd, symmetric function about $\alpha = 0$ (even for cambered sections). Thus c_ℓ for large negative angles is given by the above equations, except that the sign of c_ℓ is reversed:

$$c_\ell = -1.1 + 1.78[0.01745|\alpha| - 0.7853]^2 , \quad -90° \geq \alpha \geq -22° \tag{A12}$$

$$c_\ell = 1.1 - 1.78[0.01745|\alpha| - 2.356]^2 , \quad -160° \geq \alpha \geq -90° \tag{A13}$$

$$c_\ell = 0.763 , \quad -172.5° \geq \alpha \geq -160° \tag{A14}$$

$$c_\ell = 5.82[\pi - 0.01745|\alpha|] , \quad -180° \geq \alpha \geq -172.5° \tag{A15}$$

Equations (A8) through (A15) are assumed to hold for all airfoil sections, regardless of camber, thickness, M, or R_N.

Due to the meager amount of test data for c_ℓ above stall, the section lift coefficient is assumed to be a straight line between $c_{\ell_{max}}$ and $\alpha = 22°$. Then, from equation (A8),

$$c_\ell = 0.813 + \frac{c_{\ell_{max}} - 0.813}{22 - \alpha_{stall}} (22 - \alpha) , \quad \alpha_{stall} \leq \alpha \leq 22° , \tag{A16}$$

where it is assumed that $c_{\ell_{max}}$ occurs at

$$\alpha_{stall} = \frac{c_{\ell_{max}}}{dc_\ell/d\alpha} + \alpha_0 \tag{A17}$$

If the particular airfoil section exhibits gradual stall characteristics, equation (A17) does not accurately predict the angle at which $c_{\ell_{max}}$ occurs. However, equation (A17) may still be used in equation (A16), because the purpose of the latter is to approximate the lift curve in the region between the (assumed) linear lift-curve region and the high angle of attack region ($\alpha \geq 22°$). For negative angles of attack,

$$c_\ell = -0.813 + \frac{\left(c_{\ell_{max}}\right)_{-\alpha} + 0.813}{22 + \alpha_{neg\ stall}} (22 + \alpha) , \quad -22° \geq \alpha \geq \alpha_{neg\ stall} \tag{A18}$$

where

$$\alpha_{neg\ stall} = \frac{\left(c_{\ell_{max}}\right)_{-\alpha}}{dc_\ell/d\alpha} + \alpha_0 \tag{A19}$$

APPENDIX B

DERIVATION OF DRAG COEFFICIENT EQUATIONS

SMALL ANGLE OF ATTACK

For airfoil section angle of attack less than the stall angle, section drag coefficient is essentially constant with Mach number below the drag divergence Mach number M_{DD}. Above M_{DD}, the drag rises very steeply. Thus it is assumed that

$$c_d = (c_d)_{M=0} , \quad M \le M_{DD} , \quad \alpha \le \alpha_{stall} \tag{B1}$$

$$c_d = (c_d)_{M=0} + \frac{dc_d}{dM}(M - M_{DD}) , \quad M > M_{DD} , \quad \alpha \le \alpha_{stall} \tag{B2}$$

where $(c_d)_{M=0}$, dc_d/dM, and M_{DD} are functions of section angle of attack.

Drag Coefficient at Low M

Section drag coefficient for smooth airfoils at low Mach number, with fully turbulent boundary layer (the important case for most practical applications), may be estimated (ref. 1) by

$$(c_d)_{M=0} = (c_f)\left[S_A \frac{t}{c}\left(1 + \frac{c_s}{c_F}\right) + \frac{K(0.0125\alpha_i)^{2.5}}{(c_f)_{R_N=10^6}}\right] \tag{B3}$$

Equation (B3) was derived for symmetrical airfoil sections; however, as shown by experimental data presented in reference 1, camber has a small effect on the minimum drag coefficient. Further, an inspection of the section data in reference 1 shows that minimum c_d occurs at approximately $\alpha = 0$, for both symmetrical and cambered sections. Therefore, as discussed in reference 1, the c_d vs α relation obtained for a symmetrical airfoil may be applied with good accuracy to an airfoil with the same thickness distribution but a cambered mean line. The factors S_A, t/c, c_s/c_F, and K are constants for a specific airfoil section, and are obtained from graphs provided in reference 1. Those graphs are reproduced here as figures 7 through 10. The turbulent skin friction drag coefficient is represented by

$$c_f = \frac{0.455}{\left(\log R_{N_{eff}}\right)^{2.58}} , \tag{B4}$$

reference 10. The effective R_N (ref. 1) is given by

$$R_{N_{eff}} = R_{N_0}\left(\frac{1}{2}\frac{t}{c}\right)^2 S_A , \tag{B5}$$

where R_{N_c} is based on free-stream velocity and airfoil chord, except where it is specifically taken as 6×10^6 (third term of eq. (B3)).

Drag Divergence Mach Number

The drag divergence Mach number of an airfoil section is defined as the Mach number for which $(dc_d/dM) = 0.1$ as airspeed is increased at constant section angle of attack. Measured drag divergence Mach numbers for several airfoil sections are presented in figure 11. The M_{DD} data points in figure 11 have been fitted with straight lines, or combinations of two straight lines in the cambered airfoil cases. Correlation is very good for the NACA 4-digit, 5-digit, 65-series, and Wortmann airfoils, throughout the α range for which data were available. However, the data for the NACA 63A-series airfoils have a shift to different straight-line segments above about 5° angle of attack. Also, the NACA 64A-series data appear to have an abrupt fluctuation at about $\alpha = 10°$. It was not established whether a general trend of 6-series airfoils is represented by these data (itso note that the NACA 65_3-215 data are well represented by a straight line). Since a general expression was desired, it was assumed that M_{DD} can be represented by equations of the form

$$M_{DD} = A + B\alpha , \qquad \alpha \le \alpha_{p_{DD}} \tag{B6}$$

$$M_{DD} = C + D\alpha , \qquad \alpha > \alpha_{p_{DD}} \tag{B7}$$

where $\alpha_{p_{DD}}$ is the peak of the M_{DD} data. For symmetrical sections, $\alpha_{p_{DD}}$ is zero, C = A, and D = -B. Study of experimental data in references 3 and 4 indicates that M_{DD} is never less than 0.3, regardless of angle of attack.

Slope of c_d Curve Above M_{DD}

The slope of the c_d curve above M_{DD} was measured from experimental data for several airfoil sections, and the results are presented in figure 12. The curves plotted in the figure were obtained from least-squares curve fits of the experimental data. The 4-digit series airfoils are easily represented by curves of the form

$$\frac{dc_d}{dM} = A + B\alpha + C\alpha^2$$

However, the trend of (dc_d/dM) is more complex for the other two sections studied. Curve fits of the form

$$\frac{dc_d}{dM} = A + B\alpha + C\alpha^2 + D\alpha^3$$

were required to duplicate the rise and then leveling-off of the experimental data. Note that the quadratic equations will turn upwards, and the cubic

equations downward, at high α. Therefore, it is necessary to use a cutoff, α_c, above which (dc_d/dM) is assumed to be constant:

$$\frac{dc_d}{dM} = A + B\alpha + C\alpha^2 + D\alpha^3 , \qquad \alpha \le \alpha_c \tag{B8}$$

$$\frac{dc_d}{dM} = \left(\frac{dc_d}{dM}\right)_{\alpha=\alpha_c} , \qquad \alpha > \alpha_c \tag{B9}$$

Experimental data for (dc_d/dM) through a significant range of negative angle of attack are not available. Therefore, it is assumed that the dc_d/dM curve is a mirror image about a reference angle, α_R. For example, for the NACA 2312 section shown in figure 12, the negative data point is chosen as α_R, and so $\alpha_R = -1°$. For symmetrical sections, $\alpha_R = 0$. Thus for angles less (more negative) than α_R, substitute

$$\alpha' = |\alpha| + 2\alpha_R , \qquad \alpha < \alpha_R \tag{B10}$$

for α in equation (B8). Also, the negative angle at which (dc_d/dM) becomes constant is

$$\alpha_c' = -\alpha_c + 2\alpha_R \tag{B11}$$

LARGE ANGLE OF ATTACK

Experimental section drag coefficients through ±180° are presented for two NACA airfoil sections in figure 13. These data are companion to the lift coefficient data in figure 6. The curve fit of the data shown in figure 13 is given by

$$c_d = 2.18(|\sin\alpha|)^{1.3} , \qquad 15° \le |\alpha| \le 180° \tag{B12}$$

The lower limit of 15° for equation (B12) is arbitrary, but reflects the fact that the effects of section type and of Mach number are significant only for small α. Equation (B12) was obtained from reference 1, but the constant factor has been increased slightly to provide better correlation with the experimental data in figure 13. Equation (B12) is assumed to be applicable to all airfoil sections, regardless of section thickness, Reynolds number or Mach number.

If section angle of attack is greater than α_{stall}, but less than 15°, the drag coefficient is assumed to be a straight line between α_{stall} and 15°:

$$c_d = 0.219 - \frac{0.219 - (c_d)_{\alpha_{stall}}}{15 - |\alpha_{stall}|}(15 - |\alpha|) , \qquad \alpha_{stall} < |\alpha| < 15° \tag{B13}$$

where α_{stall} is assumed to be the angle for $c_{\ell_{max}}$:

$$\alpha_{stall} = \frac{c_{\ell_{max}}}{dc_\ell/d\alpha} + \alpha_0 \qquad \text{(B14)}$$

For negative angle of attack, $c_{\ell_{max}}$ in equation (B14) is replaced by $(c_{\ell_{max}})_{-\alpha}$.

APPENDIX C

DERIVATION OF MOMENT COEFFICIENT EQUATIONS

SMALL ANGLE OF ATTACK

The variation of airfoil section pitching moment (about the quarter-chord) with Mach number is small below the moment divergence Mach number, and may be neglected in that region. Also the moment is essentially independent of Reynolds number. For most airfoils, the slope of the moment coefficient curve is approximately constant (often zero) with angle of attack until the stall angle is reached, whereupon c_m breaks sharply. Therefore, it is assumed that

$$c_m = c_{m_0} + \frac{dc_m}{d\alpha}(\alpha) , \qquad M \le M_{MD} , \qquad |\alpha| \le \alpha_{stall} \tag{C1}$$

where c_{m_0} is c_m at $\alpha = 0$. At positive stall, c_m breaks in the negative (nose-down) c_m direction. At negative stall, the reverse is true.

Moment Divergence Mach Number

An inspection of experimental airfoil section pitching moment coefficient plotted against Mach number (e.g., ref. 4) shows that, at a fixed angle of attack, c_m is essentially constant with M until a certain M is reached, whereupon c_m diverges rapidly with further increases in M. A pitching moment divergence Mach number is defined such that M_{MD} is the Mach number for which $|dc_m/dM| = 0.5$ as airspeed is increased at constant section angle of attack. Using this definition, M_{MD} as a function of angle of attack was obtained from experimental data for several airfoil sections, and is plotted in figure 14. Although there is some scatter, the data are reasonably well fitted by straight lines, or combinations of straight lines. Therefore, M_{MD} will be represented by equations of the form

$$M_{MD} = A + B\alpha , \qquad \alpha \ge \alpha_{P_{MD}} \tag{C2}$$

$$M_{MD} = C + D\alpha , \qquad \alpha < \alpha_{P_{MD}} \tag{C3}$$

where $\alpha_{P_{MD}}$ is the peak of the data. For symmetrical sections $\alpha_{P_{MD}} = 0$, $C = A$, and $D = -B$ Experimental data in references 3 and 4 indicate that M_{MD} is always greater than about 0.3, for any angle of attack.

Above Stall or M_{MD}

There are very few data available for pitching moment above stall or M_{MD}, and no general trends are discernable. It is assumed that c_m varies linearly with α between α_{stall} and 20° (assumed to be the start of the large α region). A linear relation of c_m with M is also assumed between M_{MD} and M = 0.95. At M = 0.95 it is assumed that c_m has reached the same large-α-region value of -0.077 as at α = 20°. The selection of M = 0.95 for this relation is arbitrary. Thus,

$$c_m = -0.077 + \frac{(c_m)_{\alpha_{stall}} + 0.077}{20 - \alpha_{stall}} (20 - \alpha) , \qquad 20° > \alpha > \alpha_{stall} \tag{C4}$$

$$c_m = (c_m)_{MD} - \frac{(c_m)_{MD} + 0.077}{0.95 - M_{MD}} (M - M_{MD}) , \qquad M > M_{MD} \tag{C5}$$

Note that the condition $\alpha > \alpha_{stall}$, $M > M_{MD}$ may occur, in which case equation (C4) is used to evaluate $(c_m)_{MD}$ in equation (C5). For negative angles of attack, these equations become

$$c_m = 0.077 - \frac{0.077 - (c_m)_{\alpha_{stall}}}{20 + \alpha_{stall}} (20 + \alpha) , \qquad 20° > |\alpha| > |\alpha_{stall}| \tag{C6}$$

and

$$c_m = (c_m)_{MD} - \frac{(c_m)_{MD} - 0.077}{0.95 - M_{MD}} (M - M_{MD}) , \qquad M > M_{MD} \tag{C7}$$

where α_{stall} is negative.

LARGE ANGLE OF ATTACK

Experimental section pitching moment coefficients through ±180° are presented in figure 15 for the NACA 63A012 and NACA 0012 airfoils. A curve through the data was determined in four sections, as shown in figure 15. The curve is given by

$$c_m = -0.00802 (\alpha - 20) - 0.077 , \qquad 20° \le \alpha \le 67° \tag{C8}$$

$$c_m = -0.619[\sin(0.0260\alpha - 1.26)]^{0.398} , \qquad 67° < \alpha \le 162° \tag{C9}$$

$$c_m = -0.00838(\alpha - 162) - 0.320 , \qquad 162° < \alpha \le 170° \tag{C10}$$

$$c_m = 0.0387 (\alpha - 170) - 0.387 , \qquad 170° < \alpha \le 180° \tag{C11}$$

The lower limit of 20° for these large-angle equations is arbitrary.

Section pitching moment at large angle of attack is assumed to be an odd, symmetric function about $\alpha = 0$, even for cambered sections. Thus c_m for large negative angles is given by the above equations, except that the sign of c_m is reversed (c_m is positive)

$$c_m = 0.00802(|\alpha| - 20) + 0.077 , \quad -57° \leq \alpha \leq -20° \tag{C12}$$

$$c_m = 0.619\{\sin(0.0260|\alpha| - 1.26)\}^{0.398} , \quad -162° \leq \alpha < -67° \tag{C13}$$

$$c_m = 0.00838(|\alpha| - 162) + 0.320 , \quad -170° \leq \alpha < -162° \tag{C14}$$

$$c_m = -0.0387(|\alpha| - 170) + 0.387 , \quad -180° \leq \alpha < -170° \tag{C15}$$

APPENDIX D

COMPUTER PROGRAM FOR EVALUATION OF AIRFOIL SECTION AERODYNAMIC CHARACTERISTICS

A digital computer program was written to allow rapid evaluation of the airfoil section force and moment coefficient equations presented in this report. The program calculates section lift, drag, and pitching moment coefficients for angles of attack from -180° to +180°, and for a range of Mach numbers (M = 1.0) which may be selected by the user. Input parameters for the specific airfoil type under study are required. Sample input for the NACA 23012 airfoil section is presented in table 2. Calculated output is in the form of lift coefficient, drag coefficient, and pitching moment coefficient tables. In each table, the calculated coefficient is printed as a function of section angle of attack and of Mach number. Calculated aerodynamic coefficients for the NACA 23012 are plotted in figures 2 and 3. These data were calculated by the program as a result of the input data shown in table 2. A FORTRAN listing of the computer program is presented in this appendix.

```
C     ***  THIS PROGRAM CALCULATES AIRFOIL SECTION LIFT, DRAG, AND
C          PITCHING MOMENT COEFFICIENT TABLES AS A FUNCTION OF
C          MACH NUMBER AND ANGLE OF ATTACK  ***
C
      DIMENSION CL(120, 12), CD(120, 12), CM(120, 12), PMACH(12),
     1          ALPHA(120), AFOSGN(4)
C
C                    READ INPUTS
      READ(5,3000) AFOSGN
 3000 FORMAT(4A4)
      READ(5,3010) NMAP, SMACH, DMACH, TC, RNC, CLAI, AMACH1,
     1 ALFZ1, AMACH2, ALFZ2, C1, C2, C3, C4, C5, C6, C7, C8,
     2 C9, C10, C1N, C2N, C3N, C4N, C5N, C6N, C7N, C8N, C9N,
     3 C10N, RLC, SSM, CSCF, FK, AMCL, BMCL, CMCD, DMCD,
     4 ALFPCL, ALFCUT, ALFREF, ACCM, BCCM, CCCM, DCCM,
     5 AMMD, BMMD, CMMD, DMMD, ALFFMC, CMC, DCMCM
 3010 FORMAT(I3, 7X, 3F10.2, F10.0/ 5F10.2/ 8F10.2/ 2F10.2/ 8F10.2/
     1 2F10.2/ 4F10.2/ 4F10.2/ 3F10.2/ 4F10.2/ 4F10.2/ 3F10.2)
C
C                    PRINT OUT INPUTS
      WRITE(6,4000) AFOSGN
 4000 FORMAT(1H1// 20X, 'INPUT DATA FOR AIRFOIL SECTION: ', 4A4)
      WRITE(6,4010) NMAP, SMACH, DMACH, TC, RNC, CLAI, AMACH1,
     1 ALFZ1, AMACH2, ALFZ2, C1, C2, C3, C4, C5, C6, C7, C8,
     2 C9, C10, C1N, C2N, C3N, C4N, C5N, C6N, C7N, C8N, C9N, C10N
 4010 FORMAT(/1H0, I2, '*NMAP=', I4, T16, 'SMACH=', F5.2, T31, 'DMACH=',
     1 F5.2, T46, 'TC=', F6.3, T61, 'RNC=',1PE12.2//T2, 'CLAI=', 0PF6.3,
     2 T46, 'AMACH1=', F5.2, T61, 'ALFZ1=', F7.2, T76, 'AMACH2=', F5.2,
     3 T91, 'ALFZ2=', F7.2//T2, 'C1=', 1PE10.3, T16, 'C2=', E10.3, T31,
     4 'C3=', E10.3, T46, 'C4=', E10.3, T61, 'C5=', E10.3, T76, 'C6=',
     5 E10.3, T91, 'C7=', E10.3, T106, 'C8=', E10.3//T2, 'C9=', E10.3,
     6 T46, 'C10=', E10.3//T2, 'C1N=', E9.2, T16, 'C2N=', E10.3, T31,
     7 'C3N=', E10.3, T46, 'C4N=', E10.3, T61, 'C5N=', E10.3, T76,
     8 'C6N=', E10.3, T91, 'C7N=', E10.3, T106, 'C8N=', E10.3//T2,
     9 'C9N=', E9.2, T16, 'C10N=', E9.2)
      WRITE(6,4020) RLC, SSM, CSCF, FK, AMCL, BMCL, CMCD, DMCD,
     1 ALFPCL, ALFCUT, ALFREF, ACCM, BCCM, CCCM, DCCM,
     2 AMMD, BMMD, CMMD, DMMD, ALFFMC, CMC, DCMCM
 4020 FORMAT(/1H0, T1, ' RLC=', F7.3, T30, 'SSM=', F6.2, T51, 'CSCF=',
     1 F7.3, T90, 'FK=', F6.2// T1, ' AMCL=', 1PE10.3, T31, 'BMCL=',
     2 E10.3, T61, 'CMCD=', E10.3, T91, 'DMCD=', E10.3// T1, ' ALFPCL=',
     3 0PF6.1, T30, 'ALFCUT=', F6.1, T51, 'ALFREF=', F6.1// T1, ' ACCM=',
     4 1PE10.3, T31, 'BCCM=', E10.3, T61, 'CCCM=', E10.3, T91, 'DCCM=',
     5 E10.3// T1, ' AMMD=', E10.3, T31, 'BMMD=', E10.3, T61, 'CMMD=',
     6 E10.3, T91, 'DMMD=', E10.3// T1, ' ALFFMC=', 0PF6.1, T30, 'CMC=',
```

```
0004600C      7 FORMAT(10X, T31, 'CLMLA=', E16.8)
0004700C
0004800C                    CONSTANTS
0004900C          PIE=3.14159
0005000C          RNEFF=0.5*RNC*RLC*SQRT(SSA)
0005100C          CSF=0.455/(ALOG10(RNEFF))**2.58
0005200C          RNEFFO=3.0E6*RLC*SQRT(SSA)
0005300C          CSFO=0.455/(ALOG10(RNEFFO))**2.58
0005400C
0005500C                    SET UP ANGLE OF ATTACK
0005600C          M=0
0005700C          ALFA=-181.0
0005825  1300 ALFA=ALFA+1.0
0005918       AALFA=ABS(ALFA)
0006200C      ALFAR=0.01745*AALFA
0006300C          M=M+1
0006400C
0006500C             *** HIGH ANGLE OF ATTACK RANGE  ***
0006600C          IF(AALFA.LT.22.) GO TO 900
0006700C
0006800C                    LIFT COEFFICIENT
0006900C          IF(ALFA.GE.22..AND.ALFA.LT.90.)CLFA=1.1-1.78*(ALFAR-0.7853)**2
0006925       IF(ALFA.EQ.90.) CLFA=0.0
0007000C          IF(ALFA.GT.90..AND.ALFA.LT.160.) CLFA=-1.1+1.78*(ALFAR-2.3562)**2
0007100C          IF(ALFA.GE.160..AND.ALFA.LT.172.5) CLFA=-0.763
0007200C          IF(ALFA.GE.172.5.AND.ALFA.LT.180.) CLFA=-5.82*(PIE-ALFAR)
0007225       IF(AALFA.EQ.180.) CLFA=0.0
0007300C          IF(ALFA.LT.-22..AND.ALFA.GT.-90.) CLFA=-1.1+1.78*(ALFAR-0.7853)**2
0007325       IF(ALFA.EQ.-90.) CLFA=0.0
0007400C          IF(ALFA.LT.-90..AND.ALFA.GE.-160.) CLFA=1.1-1.78*(ALFAR-2.3562)**2
0007500C          IF(ALFA.LT.-160..AND.ALFA.GE.-172.5) CLFA=0.763
0007600C          IF(ALFA.GE.-172.5.AND.ALFA.GT.-180.) CLFA=5.82*(PIE-ALFAR)
0007700C
0007800C                    AXIAL COEFFICIENT
0007900C      900 IF(AALFA.LT.15.) GO TO 910
0008000C          CLMA = 2.18*(SIN(ALFAR))**1.7
0008100C
0008200C                    MOMENT COEFFICIENT
0008300C      910 IF(AALFA.LT.20.) GO TO 920
0008400C          IF(ALFA.GE.20..AND.ALFA.LE.87.) CMFA=-.00802*(ALFA-20.)-0.077
0008500C          IF(ALFA.LT.87..AND.ALFA.LE.162.) CMFA=-0.819*(SIN(.020*ALFA-1.22)
0008600C         1**0.596
0008700C          IF(ALFA.GT.162..AND.ALFA.LE.170.) CMFA=-.00838*(ALFA-162.)-0.322
0008800C          IF(ALFA.GT.170..AND.ALFA.LE.180.) CMFA=.0307*(ALFA-170.)-0.307
0008900C          ALFAR=AALFA
```

```
      IF(ALFA.GE.-67..AND.ALFA.LE.-20.) CMFA=.0080*(ALFAA-20.)+0.077
      IF(ALFA.GE.-102..AND.ALFA.LT.-67.) CMFA=0.619*(SIN(.020*ALFAA
     1 -1.26))**0.96
      IF(ALFA.GE.-170..AND.ALFA.LT.-102.) CMFA=.0080*(ALFAA-102.)+0.320
      IF(ALFA.GE.-180..AND.ALFA.LT.-170.) CMFA=-.0287*(ALFAA-170.)+0.387
  920 IF(ALFA.LE.22.) GO TO 1210

          ***  LOW ANGLE OF ATTACK RANGE  ***

                CRAG COEFFICIENT AT ZERO MACH NUMBER
      IF(ALFA.LE.15.) GO TO 1000
      ALFARE=ALFAR
      IF(ALFAR.LT..0001) ALFARE=.0001
      CDM2=CSF*(CSA*RLC*(1.+CSCF)+(FK*ALFARE**2.7)/CSF6)

                CRAG DIVERGENCE MACH NUMBER
      IF(ALFA.GE.ALFPOS) DUMN=AMCL+BMCL*ALFA
      IF(ALFA.LT.ALFPOS) DUMN=CMCL+DMCL*ALFA
      IF(DUMN.LT.0.3) DUMN=0.3

                SLOPE OF CL CURVE ABOVE CRAG DIVERGENCE
      IF(ALFA.GE.ALFREF.AND.ALFA.LE.ALFCUT) DCLDM=ACLM+BCLM*ALFA+CCLM
     1 *ALFA**2+DCLM*ALFA**3
      IF(ALFA.GT.ALFCUT) DCLDM=ACLM+BCLM*ALFCUT+CCLM*ALFCUT**2
     1 +DCLM*ALFCUT**3
      IF(ALFA.GE.ALFREF) GO TO 1000
      ALFPRM=2.0*ALFREF-ALFA
      ALCUTP=2.0*ALFREF-ALFCUT
      IF(ALFA.GE.ALCUTP) DCLDM=ACLM+BCLM*ALFPRM+CCLM*ALFPRM**2
     1 +DCLM*ALFPRM**3
      IF(ALFA.LT.ALCUTP) DCLDM=ACLM+BCLM*ALFCUT+CCLM*ALFCUT**2
     1 +DCLM*ALFCUT**3

                MOMENT DIVERGENCE MACH NUMBER
 1000 IF(AMLFA.GE.20.) GO TO 1010
      IF(ALFA.GE.ALFPMO) AMDMN=AMPL+BMPL*ALFA
      IF(ALFA.LT.ALFPMO) AMDMN=CMPL+DMPL*ALFA
      IF(AMDMN.LT.0.3) AMDMN=0.3

                MACH NUMBER LOOP
 1010 AMACH=SMACH
      DO 1200 N=1,NMACH

                LIFT CURVE SLOPE
      AMU=1.0/SQRT(1.0-AMACH**2)
```

```
0013300C       CLA=CLA1*(AMU+TC/(1.+TC)*(AML*(AML-1.)+0.6*(AMU**2-1.)**2))
0013400C       IF(AMACH.GT.AMACH1) CLA=CLA-0.45*(AMACH-AMACH1)
0013500C       IF(CLA.LE.0.05) CLA=0.05
0013600CC
0013700CC                  ANGLE OF ZERO LIFT
0013800C       ALFZ=ALFZ1
0013900C       IF(AMACH.GT.AMACH1) ALFZ=ALFZ1-(ALFZ1-ALFZ2)/(AMACH1-AMACH2)
0014000C      1 *(AMACH1-AMACH)
0014100CC
0014200CC                  MAXIMUM LIFT COEFFICIENT
0014300C       BMACH=AMACH
0014425        IF(BMACH.LT..001) BMACH=.001
0014500C       IF(ALFA.LE.0.0) GO TO 1110
0014600C       CLMAX=C1N+C2N*BMACH+C3N*BMACH**2+C4N*BMACH**3+C5N*BMACH**4
0014700C      1 +(C6N+C7N*BMACH**C8N)*SIN(C9N+C10N*BMACH)
0014800C       GO TO 1120
0014900C  1110 CLMAX=C1+C2*BMACH+C3*BMACH**2+C4*BMACH**3+C5*BMACH**4
0015000C      1 +(C6+C7*BMACH**C8)*SIN(C9+C10*BMACH)
0015100CC
0015200CC                  ANGLE OF ATTACK FOR MAX CL
0015300C  1120 ALFCLM=CLMAX/CLA+ALFZ
0015400C       ALFSTL=ALFCLM
0015500CC
0015600CC                  LIFT COEFFICIENT
0015700C       IF(ABALFA.GT.ABS(ALFCLM)) GO TO 1130
0015800C       CL(M,N)=CLA*(ALFA-ALFZ)
0015900C       GO TO 1140
0016000C  1130 IF(ALFA.GE.0.0) CL(M,N)=0.813+(CLMAX-0.813)/(22.-ALFCLM)*(22.
0016100C      1 -ALFA)
0016200C       IF(ALFA.LT.0.0) CL(M,N)=-0.813+(CLMAX+0.813)/(22.+ALFCLM)*(22.
0016300C      1 +ALFA)
0016400CC
0016500CC                  DRAG COEFFICIENT
0016600C  1140 IF(AMACH.GE.1.5) GO TO 1160
0016700C       IF(ABALFA.GT.ABS(ALFSTL)) GO TO 1150
0016800C       IF(AMACH.LE.DUMN) CD(M,N)=CDMZ
0016900C       IF(AMACH.GT.DUMN) CD(M,N)=CDMZ+DCDDM*(AMACH-DUMN)
0017000C       GO TO 1160
0017100C  1150 CDMAS=CSF*(SSA*RLC*(1.+CSCF)+(FK*(.01745*ABS(ALFSTL))**2.7)/CSF6)
0017200C       IF(ALFSTL.GE.ALFPCD) CDMAS=AMCD+BMCD*ALFSTL
0017300C       IF(ALFSTL.LT.ALFPCD) CDMAS=CMCD+DMCD*ALFSTL
0017400C       IF(CDMAS.LT.0.3) CDMAS=0.3
0017500C       IF(ALFSTL.GE.ALFREF.AND.ALFSTL.LE.ALFCUT) CCDDMS=ACDM+BCDM*ALFSTL
0017600C      1 +CCDM*ALFSTL**2+DCDM*ALFSTL**3
0017700C       IF(ALFSTL.GT.ALFCUT) CCDDMS=ACDM+BCDM*ALFCUT+CCDM*ALFCUT**2
```

```
0C178000      1 +CCDM*ALFCUT**3
0C179000       IF(ALFSTL.GE.ALFREF) GO TO 1165
0C180000      ALFPRM=ABS(ALFSTL)+2.0*ALFREF
0C181000       ALCUTP=2.0*ALFREF-ALFCUT
0C182000       IF(ALFSTL.GE.ALCUTP) DCDCMS=ACDM+BCDM*ALFPRM+CCDM*ALFPRM**2
0C183000      1 +DCDM*ALFPRM**3
0C184000       IF(ALFSTL.LT.ALCUTP) DCDCMS=ACDM+BCDM*ALFCUT+CCDM*ALFCUT**2
0C185000      1 +DCDM*ALFCUT**3
0C186000 1165 IF(AMACH.LE.DDMNS) CDSTL=CDMZS
0C187000       IF(AMACH.GT.DDMNS) CDSTL=CDMZS+DCDCMS*(AMACH-DDMNS)
0C188000       CL(M,N)=0.219-(0.219-CDSTL)/(15.-ABS(ALFSTL))*(15.-AALFA)
0C189000C
0C190000C                  MOMENT COEFFICIENT
0C191950  1166 IF(AALFA.GE.20.) GO TO 1200
0C193185       IF(AALFA.GT.ABS(ALFSTL)) GO TO 1170
0C193320       CM(M,N)=CMC+DCMDA*ALFA
0C194855       GO TO 1175
0C204000 1170 CMSTL=CMC+DCMDA*ALFSTL
0C205000       IF(ALFA.GE.0.0) CM(M,N)=-0.077+(CMSTL+0.077)/(20.-ALFSTL)
0C206000      1 *(20.-ALFA)
0C207000       IF(ALFA.LT.0.0) CM(M,N)=0.077-(0.077-CMSTL)/(20.+ALFSTL)
0C208000      1 *(20.+ALFA)
0C208008  1175 IF(AMACH.LE.AMDMN) GO TO 1200
0C208016       IF(ALFA.GE.0.0) CM(M,N)=CM(M,N)-(CM(M,N)+0.077)/(0.95-AMDMN)*(AMACH-AMDMN)
0C208032       IF(ALFA.LT.0.0) CM(M,N)=CM(M,N)-(CM(M,N)-.077)/(0.95-AMDMN)*(AMACH-AMDMN)
0C209000C
0C210000C                  INCREMENT MACH NUMBER
0C211000C 1200 AMACH=AMACH+DMACH
0C212000C
0C213000C                  CHANGE HIGH-ANGLE COEFFICIENTS TO SUBSCRIPTED FORM
0C214000C 1210 IF(AALFA.LT.15.) GO TO 1220
0021425        IF(ALFA.EQ.180.) GO TO 1225
0C215000C      DO 1230 N=1,NMAP
0C216000C 1230 CL(M,N)=CDMA
0021610        GO TO 1220
0021620  1225 DO 1235 N=1,NMAP
0C216300       CL(M,N)=CD(46,N)
0021640  1235 CL(M,N)=CD(46,N)
0C217000C 1220 IF(AALFA.LT.20.) GO TO 1240
0C218000C      DO 1250 N=1,NMAP
0C219000C 1250 CM(M,N)=CMFA
0C220000C 1240 IF(AALFA.LT.22.) GO TO 1260
0C221000C      DO 1270 N=1,NMAP
0C222000C 1270 CL(M,N)=CLFA
0C223000C
```

```
00224000C                    INCREMENT ANGLE OF ATTACK
00225000C 1260 PALFA(M)=ALFA
00225120       IF(ALFA.LT.-25..OR.ALFA.GE.25.) ALFA=ALFA+4.0
00225240       IF(ALFA.GE.-25..AND.ALFA.LT.-10.) ALFA=ALFA+1.5
00225360       IF(ALFA.GE.10..AND.ALFA.LT.25.) ALFA=ALFA+1.5
00226000C      IF(ALFA.LT.180.) GO TO 1300
00227000C
00228000C                    PRINT OUT RESULTS
00229000C      WRITE(6,4025)
00230000C 4025 FORMAT(1H1,30X, 'LIFT COEFFICIENT TABLE')
00231000C      AMACH=SMACH
00232000C      DO 1310 N=1,NMAP
00233000C      PMACH(N)=AMACH
00234000C 1310 AMACH=AMACH+DMACH
00235000C      WRITE(6,4030) (PMACH(N), N=1,NMAP)
00236000C 4030 FORMAT(1H , 'MACH NO=', (12F9.3))
00237000C      WRITE(6,4040)
00238000C 4040 FORMAT(1H , 'ALPHA')
00239000C      DO 1320 J=1,M
00240000C 1320 WRITE(6,4050) PALFA(J), (CL(J,N), N=1,NMAP)
00241000C 4050 FORMAT(1H , F6.1, 2X, (12F9.4))
00242000C      WRITE(6,4060)
00243000C 4060 FORMAT(1H1, 30X, 'DRAG COEFFICIENT TABLE')
00244000C      WRITE(6,4030) (PMACH(N), N=1,NMAP)
00245000C      WRITE(6,4040)
00246000C      DO 1330 J=1,M
00247000C 1330 WRITE(6,4050) PALFA(J), (CD(J,N), N=1,NMAP)
00248000C      WRITE(6,4070)
00249000C 4070 FORMAT(1H1, 30X, 'PITCHING MOMENT COEFFICIENT TABLE')
00250000C      WRITE(6,4030) (PMACH(N), N=1,NMAP)
00251000C      WRITE(6,4040)
00252000C      DO 1340 J=1,M
00253000C 1340 WRITE(6,4050) PALFA(J), (CM(J,N), N=1,NMAP)
00254000C      STOP
00255000C      END
```

REFERENCES

1. Schwartzberg, M. A.: Airfoil Profile Drag. USAAVSCOM TR 75-19, 1975.

2. Dadone, L U.: U.S. Army Helicopter Design Datcom, Volume I - Airfoils. USAAMRDL CR 76-2, 1976.

3. Abbott, I. H.; and von Doenhoff, A. E.: Theory of Wing Sections. Dover Publications, Inc., New York, N.Y., 1959.

4. Noonan, K. W.; and Bingham, C. J.: Two-Dimensional Aerodynamic Characteristics of Several Rotorcraft Airfoils at Mach Numbers from 0.35 to 0.90. NASA TM X-73990, 1977.

5. Carpenter, P. J.: Lift and Profile - Drag Characteristics of an NACA 0012 Airfoil Section as Derived from Measured Helicopter - Rotor Hovering Performance. NACA TN 4357, 1958.

6. Shivers, J. P.; and Carpenter, P. J.: Effects of Compressibility on Rotor Hovering Performance and Synthesized Blade-Section Characteristics Derived from Measured Rotor Performance of Blades Having NACA 0015 Airfoil Tip Sections. NACA TN 4356, 1958.

7. Hoffman, J. A.: Equation Summary for the Modular Stability Derivative Program, C Version. MRI Rpt 4343-3, Mechanics Research, Inc., July 1970.

8. Sipe, O. E.; and Gorenberg, N. B.: Effect of Mach Number, Reynolds Number, and Thickness Ratio on the Aerodynamic Characteristics of NACA 63A-Series Airfoil Sections. USAAML TR 65-28, 1965.

9. Critzos, C. C.; Heyson, H. H.; and Boswinkle, R. W.: Aerodynamic Characteristics of NACA 0012 Airfoil Section at Angles of Attack from 0° to 180°. NACA TN 3361, 1955.

10. Schlichting, H.: Boundary Layer Theory. McGraw-Hill, New York, N.Y., 1960.

11. Nitzberg, G. E.; and Crandall, S.: A Study of Flow Changes Associated with Airfoil Section Drag Rise at Supercritical Speeds. NACA TN 1813, 1949.

12. Summers, J. L.; and Treon, S. L.: The Effects of Amount and Type of Camber on the Variation with Mach Number of the Aerodynamic Characteristics of a 10-Percent-Thick NACA 64A-Series Airfoil Section. NACA TN 2096, 1950.

TABLE 1.- DATA REQUIREMENTS

Input data	Equation numbers
Lift coefficient	
$(dc_\ell/d\alpha)_{inc}$	(A2), (A3)
t/c	(A2), (A3), also figs. 7-10
M_1, M_2	(A3), (A4), (A5)
$(\alpha_0)_1$, $(\alpha_0)_2$	(A4), (A5)
$c_{\ell_{max}}$ coefficients	
C_1 + C_{10} for +α case	(A6)
C_1 + C_{10} for -α case	(A6)
Drag coefficient	
M_{DD} coefficients A, B, C, D	(B6), (B7)
$\alpha_{P_{DD}}$	(B6), (B7)
R_{N_0}	(B5)
dc_d/dM coefficients A, B, C, D	(B8)
α_c	(B8), (B9), (B11)
α_R	(B10), (B11)
Moment coefficient	
M_{MD} coefficients: A, B, C, D	(C2), (C3)
$\alpha_{P_{MD}}$	(C2), (C3)
c_{m_0}	(C1)
$dc_m/d\alpha$	(C1)

TABLE 2.- SAMPLE INPUT FOR NACA 23012

Symbol	FORTRAN name	Value	Symbol	FORTRAN name	Value
---	NMNP	10	L/c	RLC	2.035
---	SMACH	0	S_A	SSA	1.18
---	DMACH	.1	C_S/C_F	CSCF	.037
t/c	TC	.12	K	FK	1.55
R_{N_o}	RNO	8.10×10^6	Coefficients for M_{DD}:		
$(dc_\ell/d\alpha)_{inc}$	CLAI	.100/deg	A	AMDD	0.730
M_1	AMACH1	.80	B	BMDD	-.0246
$(\alpha_0)_1$	ALFZ1	-1.20 deg	C	CMDD	.830
M_2	AMACH2	.85	D	DMDD	.0246
$(\alpha_0)_2$	ALFZ2	-.70 deg	$\alpha_{P_{DD}}$	ALFPDD	-2.0°
Coefficients for $+c_{\ell_{max}}$:			α_c	ALFCUT	10.0°
C_1	C1	1.622	α_R	ALFREF	-2.0°
C_2	C2	.337	Coefficients for dc_d/dM:		
C_3	C3	-2.316	A	ACDM	0.274
C_4	C4	.0	B	BCDM	.0253
C_5	C5	.0	C	CCDM	.00273
C_6	C6	.0	D	DCDM	.000264
C_7	C7	.0	Coefficients for M_{MD}:		
C_8	C8	.0	A	AMMD	0.810
C_9	C9	.0	B	BMMD	-.026
C_{10}	C10	.0	C	CMMD	.910
Coefficients for $-c_{\ell_{max}}$:			D	DMMD	.026
C_1	C1N	-1.200	$\alpha_{P_{MD}}$	ALFPMD	-2.0°
C_2	C2N	-.250	c_{m_0}	CMO	-.010
C_3	C3N	1.716	$dc_m/d\alpha$	DCMDA	.0014/deg
C_4	C4N	.0			
C_5	C5N	.0			
C_6	C6N	.0			
C_7	C7N	.0			
C_8	C8N	.0			
C_9	C9N	.0			
C_{10}	C10N	.0			

TABLE 3.- MEASURED AND CALCULATED LIFT-CURVE SLOPE FOR SEVERAL AIRFOIL SECTIONS

Airfoil section	Mach number	Measured[a] $dc_l/d\alpha$ per deg	Calculated[b] $dc_l/d\alpha$ per deg	Difference, %
NACA 0012	0.30	0.103	---	---
	.40	.108	0.108	0.0
	.60	.128	.127	.8
	.80	.200	.194	-3.0
NACA 23015	.30	.100	---	---
	.40	.105	.105	.0
	.60	.120	.125	4.2
	.75	.155	.170	9.7
NACA 63A012	.30	.100	---	---
	.39	.106	.104	-1.9
	.58	.125	.121	-3.2
	.74	.160	.157	-1.9
VERTOL V23010-1.58	.30	.122	---	---
	.40	.124	.129	4.0
	.60	.145	.151	4.1
	.77	.240	.206	-14.2
VERTOL VR-7	.30	.110	---	---
	.40	.118	.115	-2.5
	.62	.138	.139	.7
	.75	.180	.178	-1.1

[a] Reference 2.

[b] Equation (A2).

TABLE 4.- MEASURED MACH NUMBER EFFECT ON AIRFOIL SECTION ANGLE OF ZERO LIFT

Airfoil section	M_1[a]	$(\alpha_0)_1$, deg	M	α_0, deg	Reference
NACA 2409-34	0.80	-2.5	0.83	-0.5	3
NACA 4409-34	.70	-4.5	.80	-1.9	3
NACA 23012	.80	-1.2	.85	-.7	2
NACA 23015	.78	-1.2	.80	-.9	2
			.83	2.0	
NACA 64A(4.5)08	.81	-3.2	.85	-2.0	2
			.90	-.9	
			.96	-.5	
NACA 64A608	.81	-4.5	.86	-2.5	2
			.90	-.9	
			.96	-.5	
NACA 64A312	.75	-2.3	.80	-2.0	2
			.85	.4	
			.90	-.2	
NACA 64612	.76	-4.5	.80	-2.6	2
			.85	-.4	
			.90	-.3	
V23010-1.58 with T.E. Tab	.77	.5	.82	.2	2
			.86	.2	
VR-7 with T.E. Tab	.75	-2.0	.82	-1.1	2
			.92	-1.7	
VR-8 with T.E. Tab	.85	-.8	.90	-.6	2
			.95	-.6	

[a] M_1 is the highest Mach number in the experimental data for which α_0 remains at a constant value.

TABLE 5.- MEASURED AND CALCULATED LOW MACH NUMBER $c_{\ell_{max}}$ FOR NEGATIVE ANGLE OF ATTACK

Airfoil section	Measured $c_{\ell_{max}}$ [a]		Measured [b] $(\Delta c_{\ell})_{\alpha=0}$	Calculated [b] $(c_{\ell_{max}})_{-}$	Error, %
	+	-			
NACA 1412	1.60	-1.20	0.15	-1.30	8.3
NACA 2412	1.70	-1.08	.26	-1.18	9.3
NACA 4412	1.64	-.78	.43	-.78	0
NACA 63_1-212	1.58	-1.18	.23	-1.12	-5.1
NACA 63_1-412	1.72	-1.00	.35	-1.02	2.0
NACA 65_1-212	1.45	-1.10	.13	-1.19	8.2
NACA 65_1-412	1.65	-.80	.35	-.95	18.8

[a] Reference 3.

[b] Equation (A7).

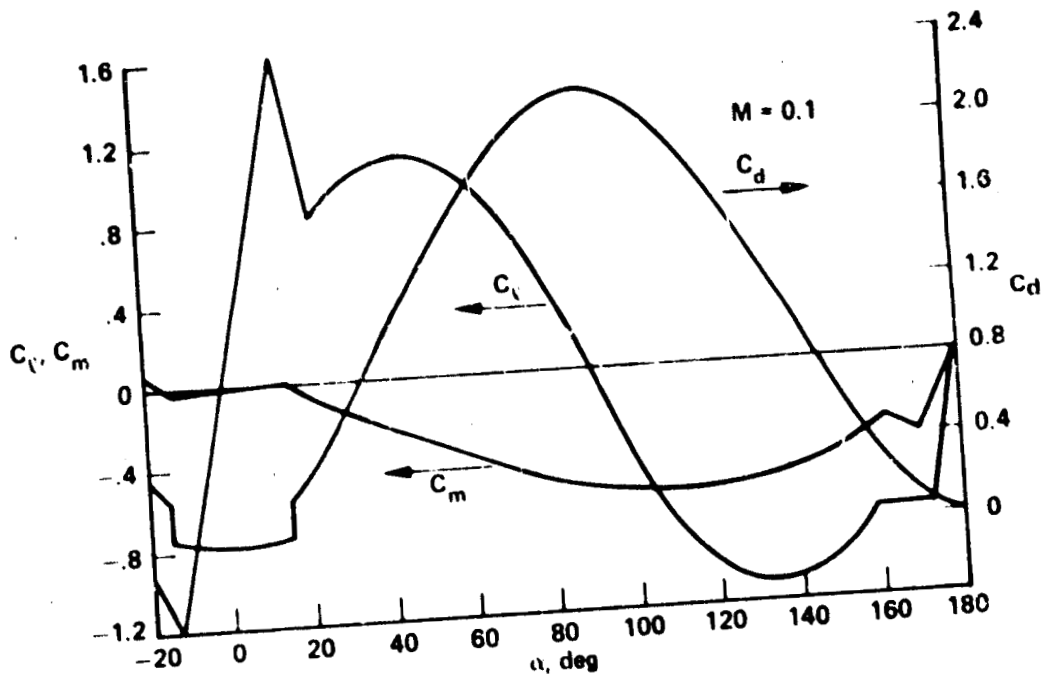

Figure 1.- Calculated lift, drag, and pitching-moment coefficients for the NACA 23012 airfoil section, at M = 0.1.

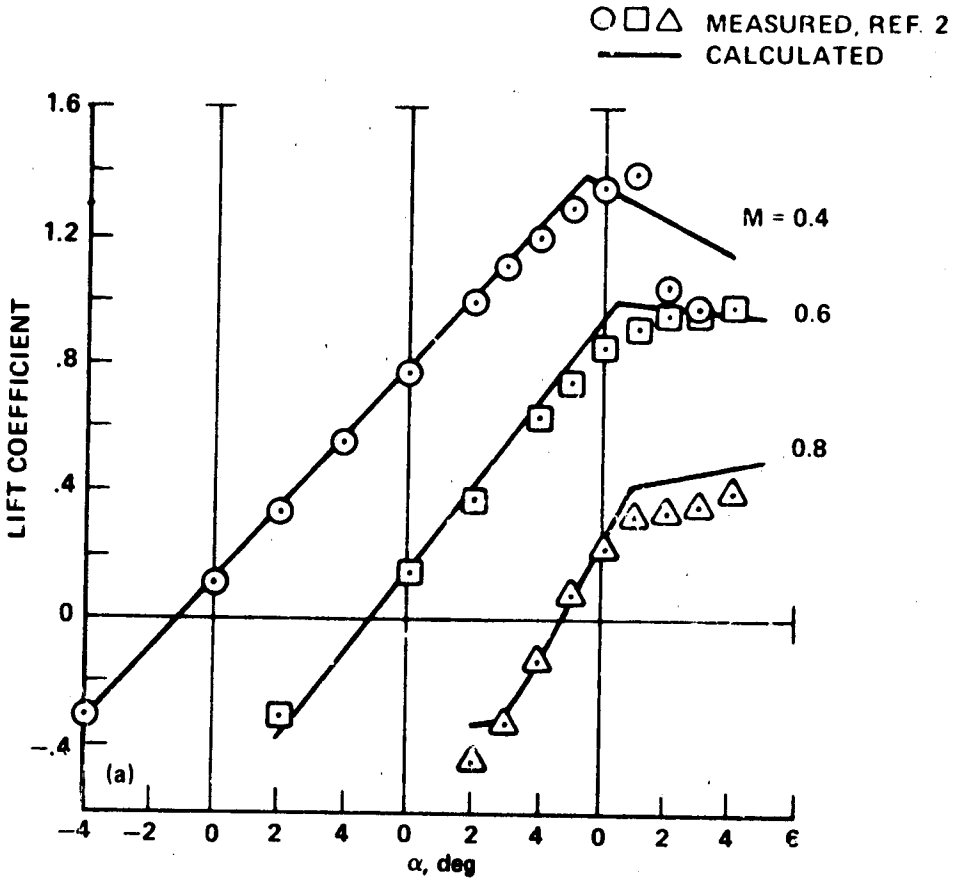

(a) Section lift coefficient.

Figure 2.- Calculated and measured aerodynamic characteristics for NACA 23012 airfoil section.

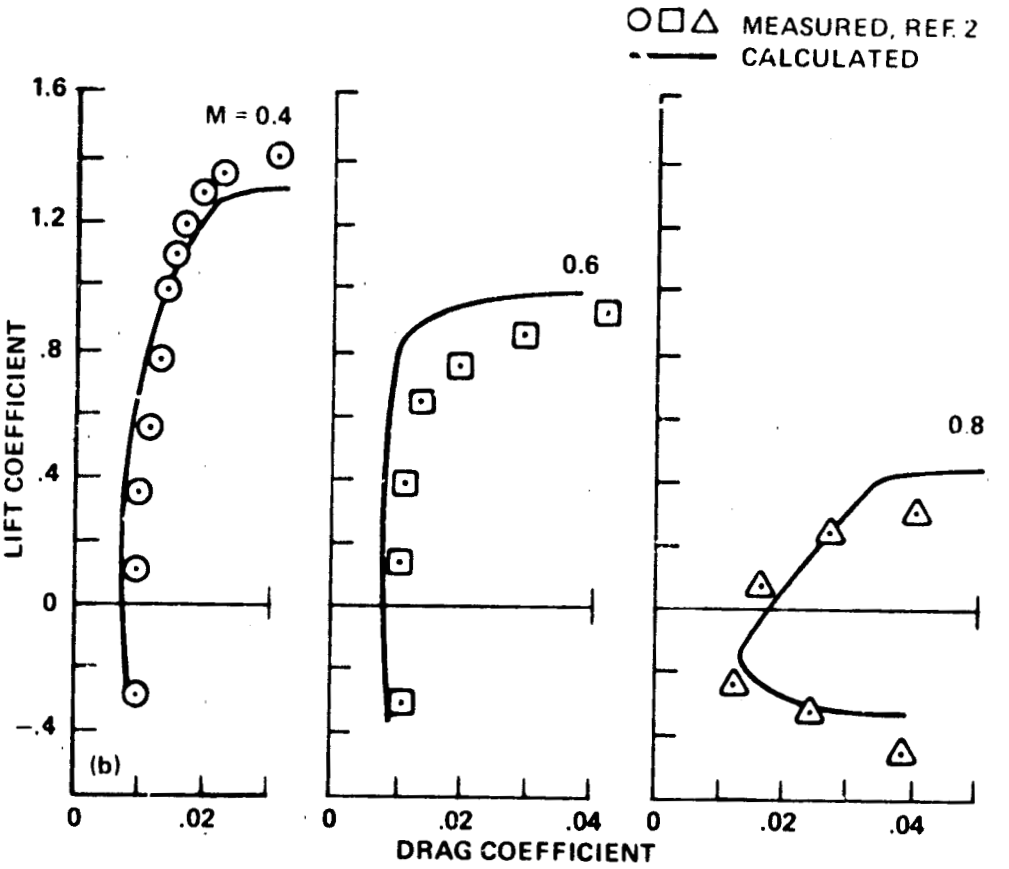

(b) Section drag coefficient.

Figure 2.- Continued.

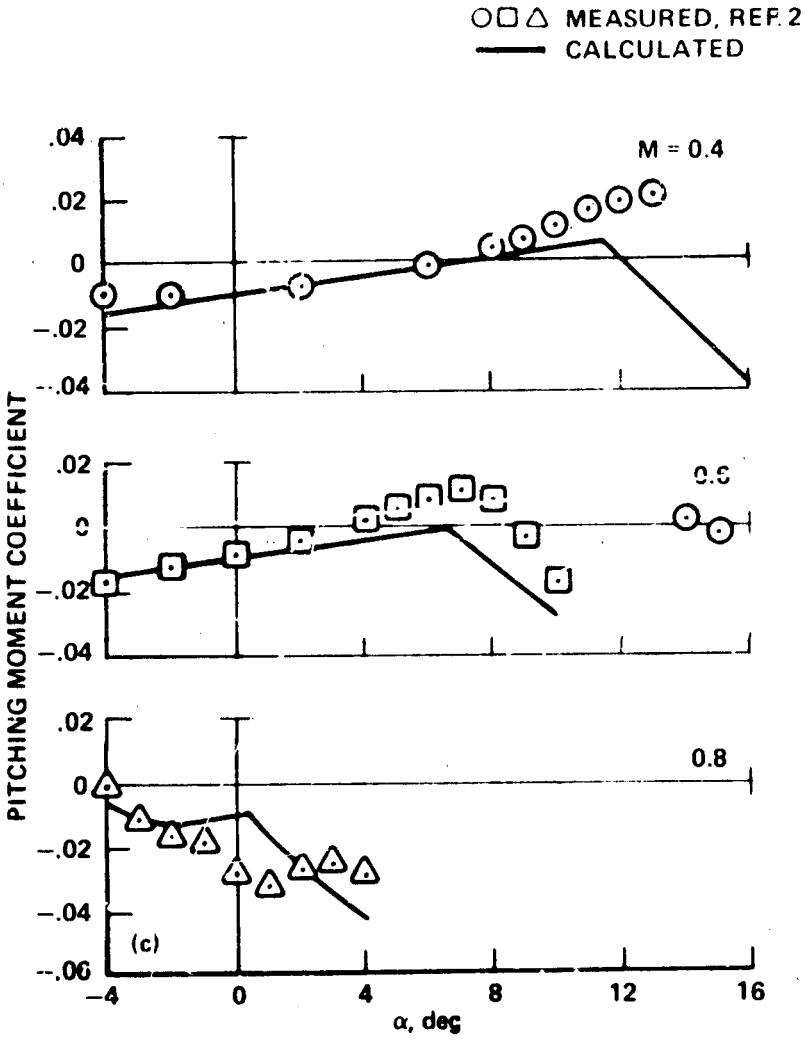

(c) Section pitching-moment coefficient.

Figure 2.- Concluded.

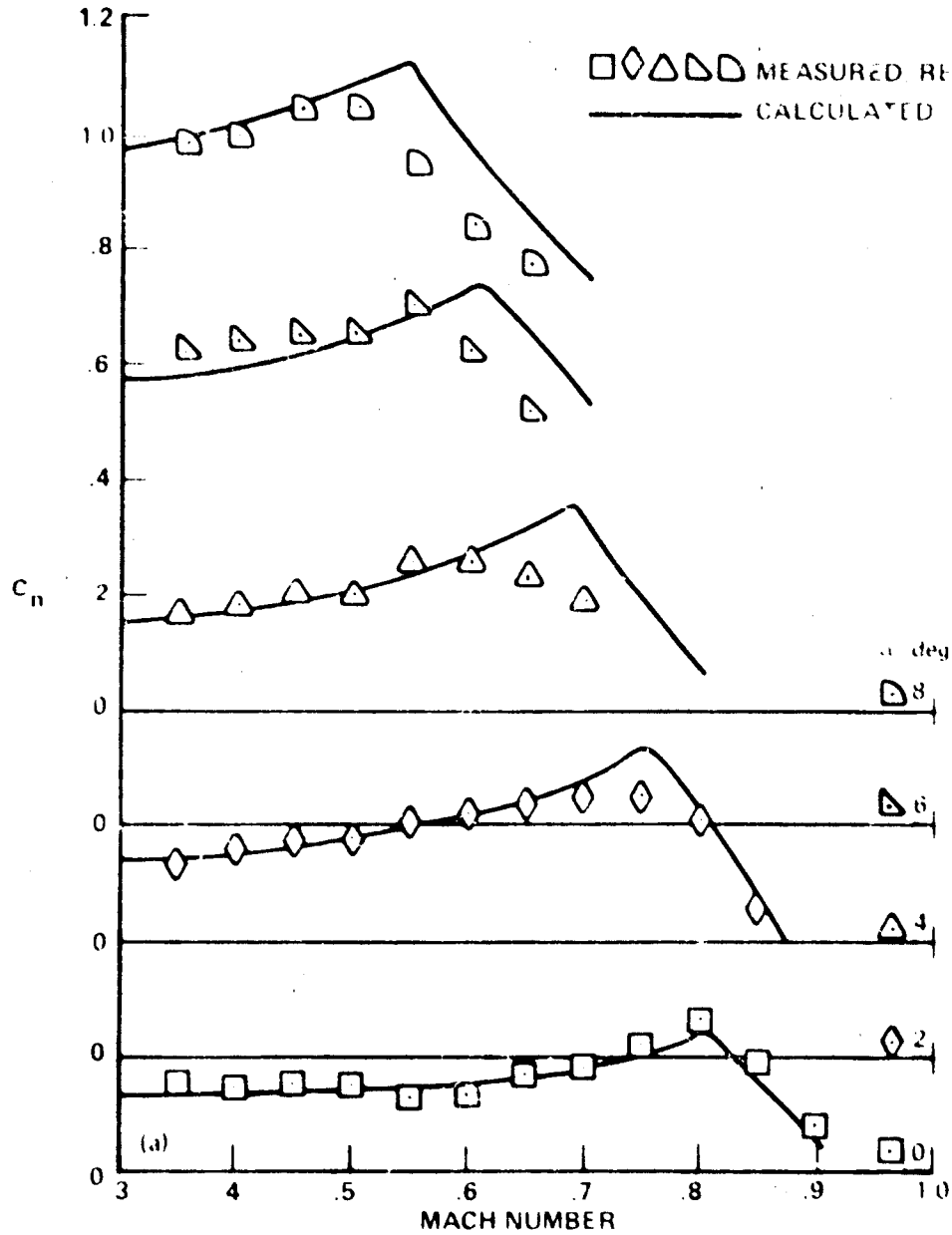

(a) Section normal force coefficient.

Figure 3.- Calculated and measured aerodynamic characteristics for NACA [illegible] airfoil section.

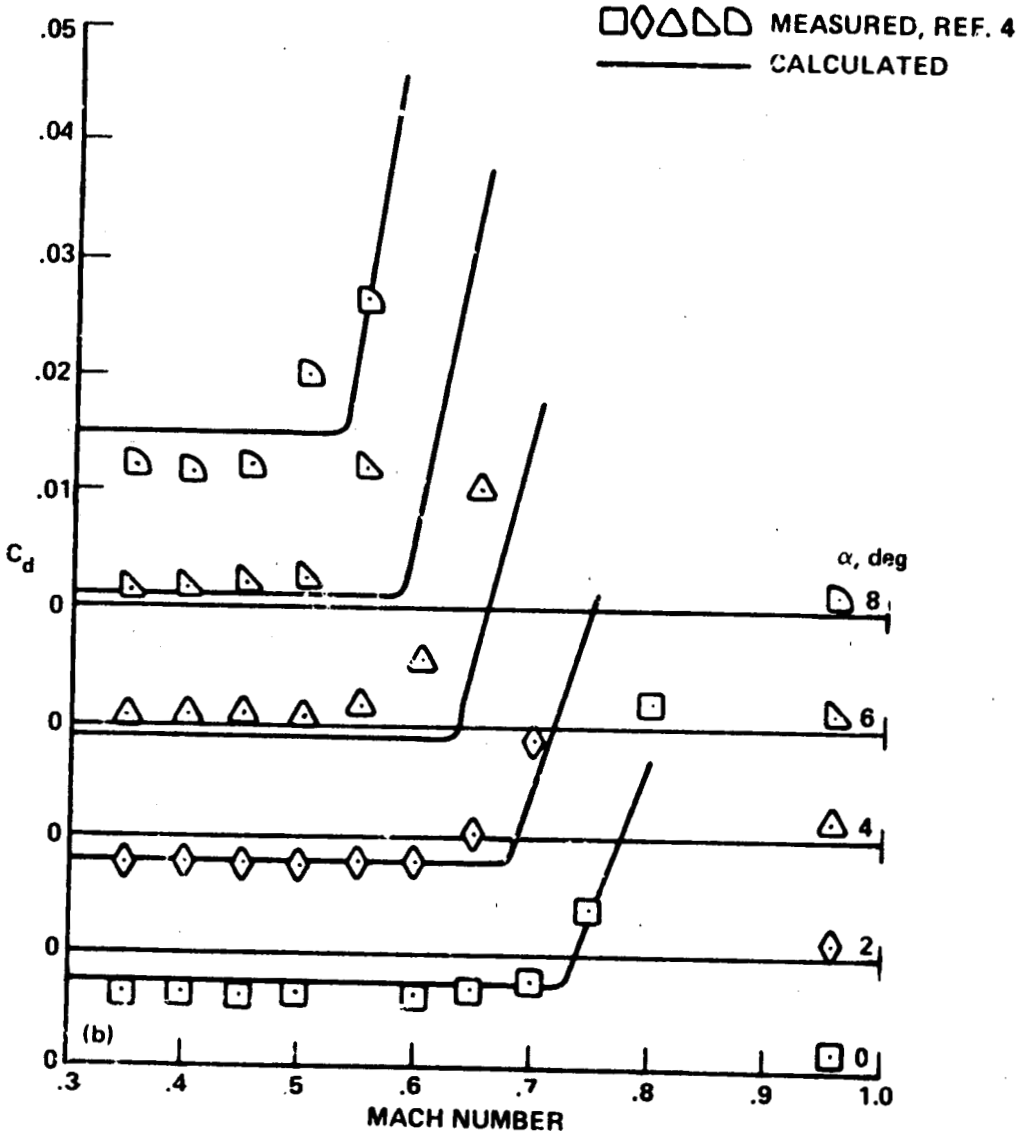

(b) Section drag coefficient.

Figure 3.- Continued.

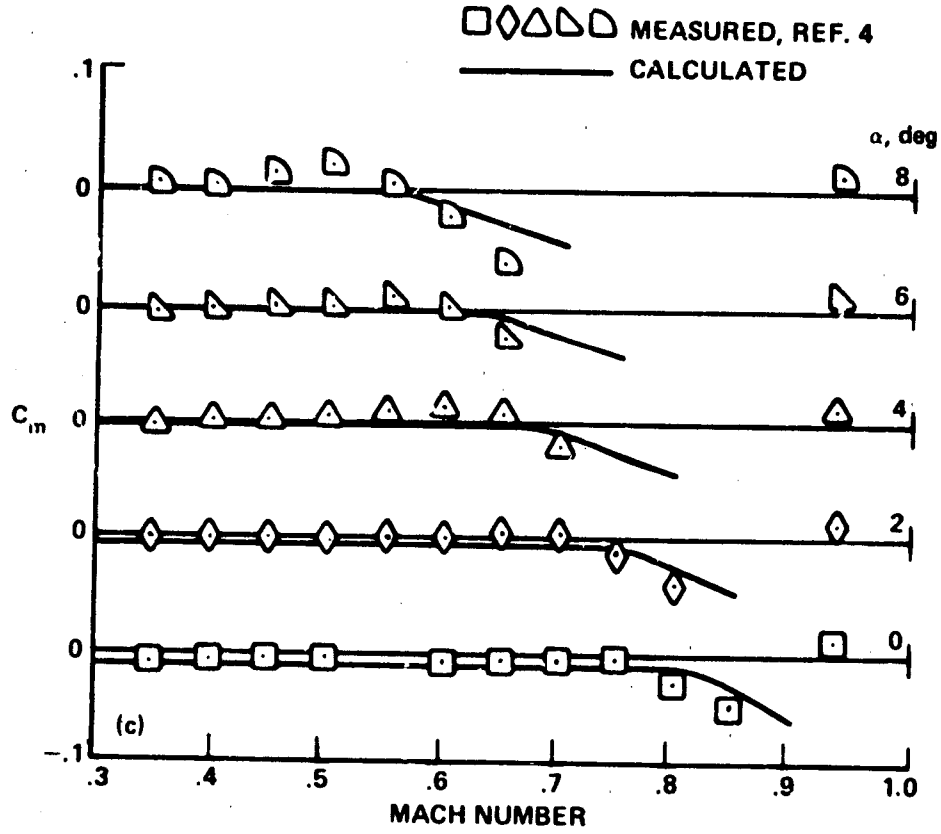

(c) Section pitching-moment coefficient.

Figure 3.- Concluded.

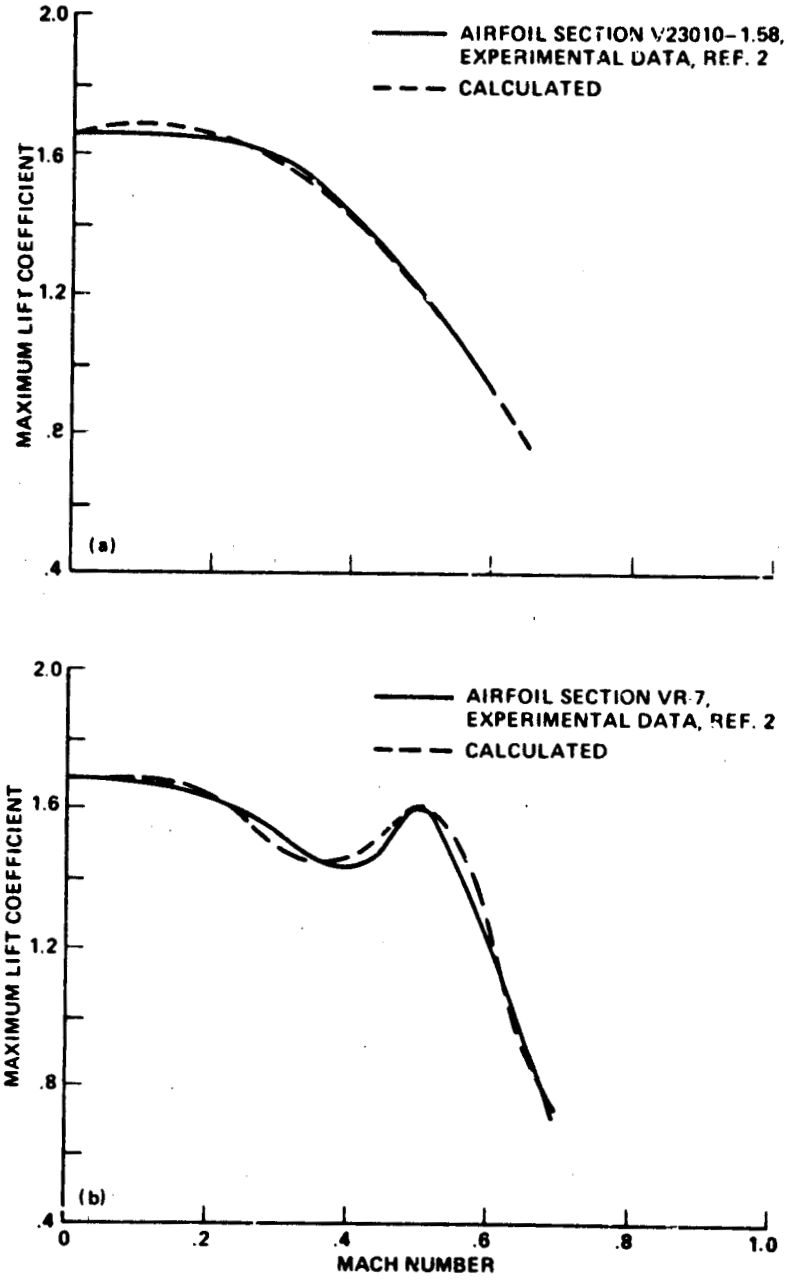

(a) Airfoil section V23010-1.58.

(b) Airfoil section VR-7.

Figure 4.- Maximum lift coefficient.

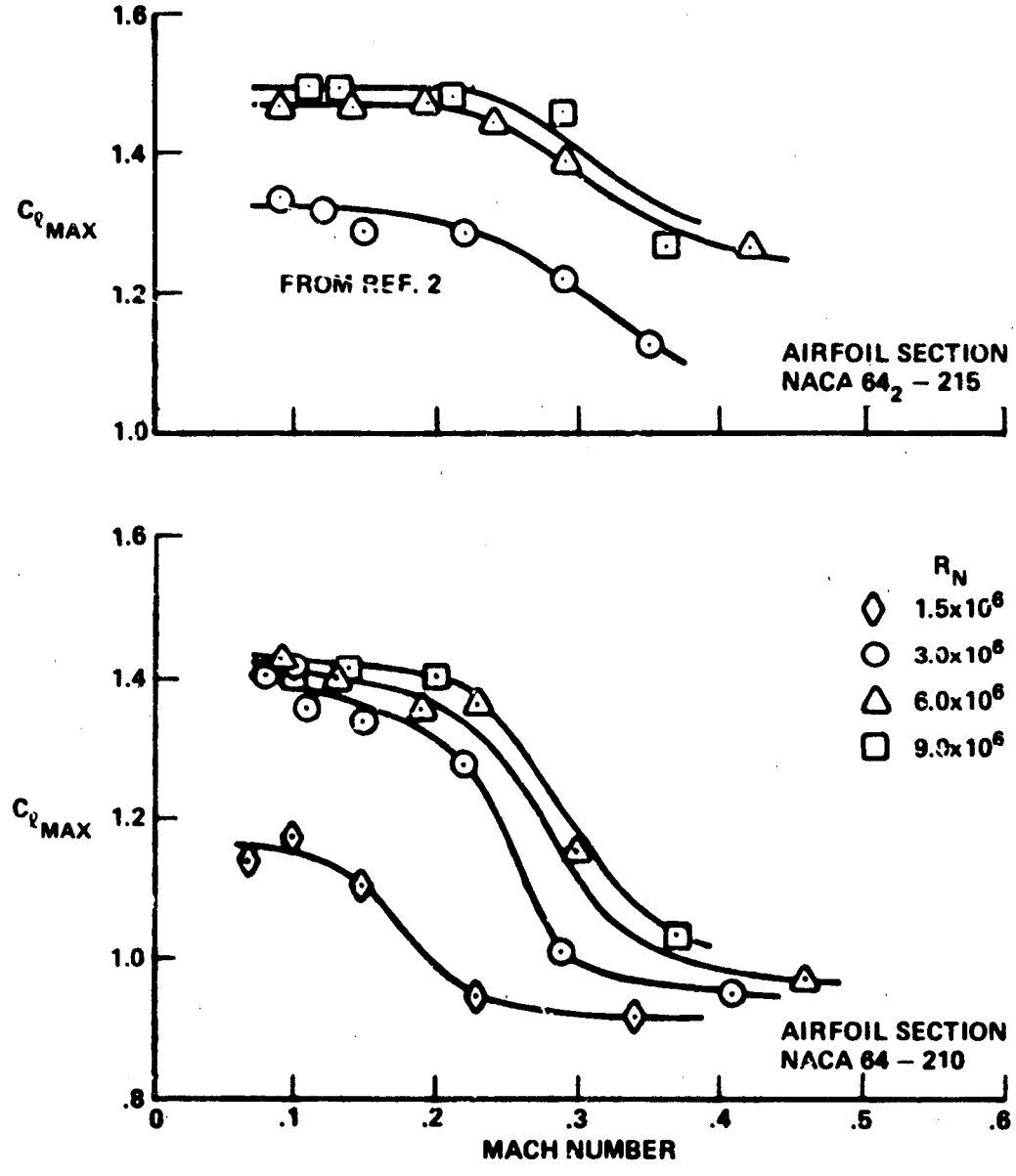

Figure 5.- Effect of Mach number and Reynolds number on airfoil section maximum lift coefficient.

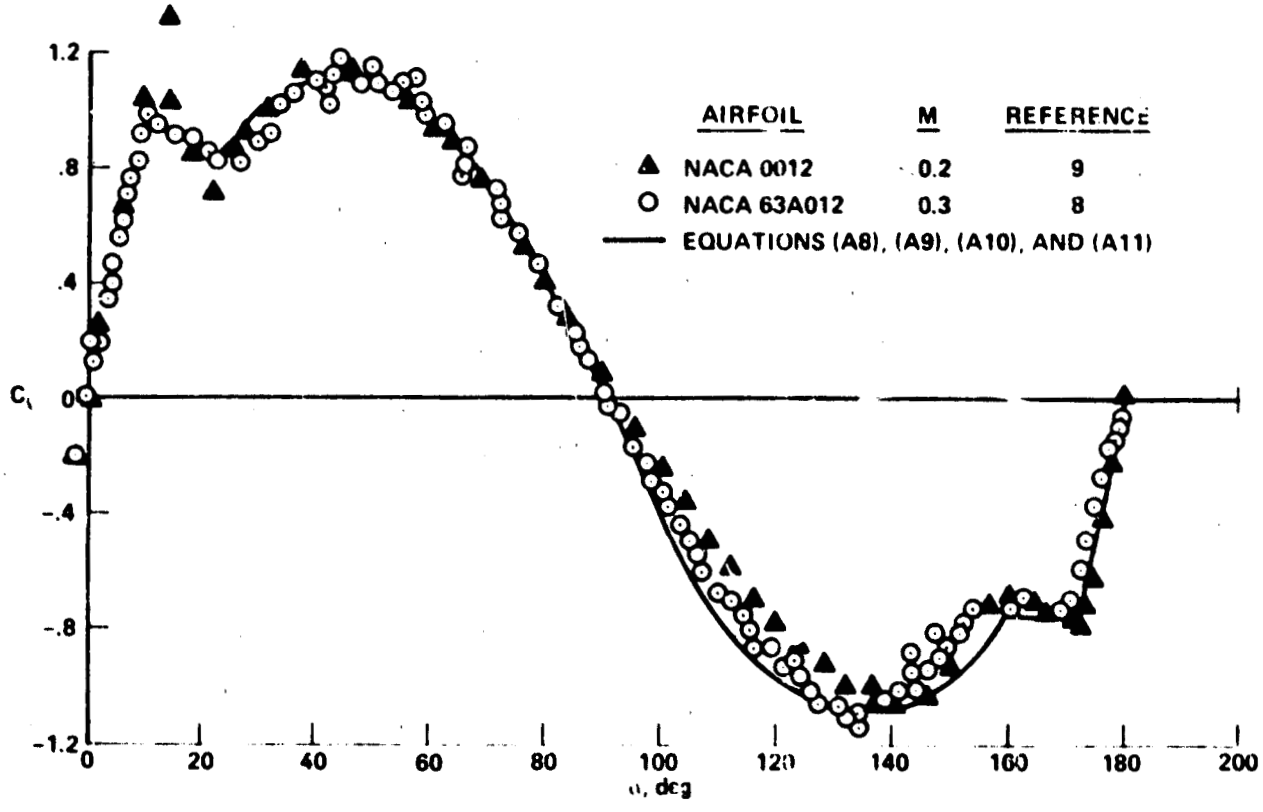

Figure 6.- Airfoil section lift coefficient through 180°.

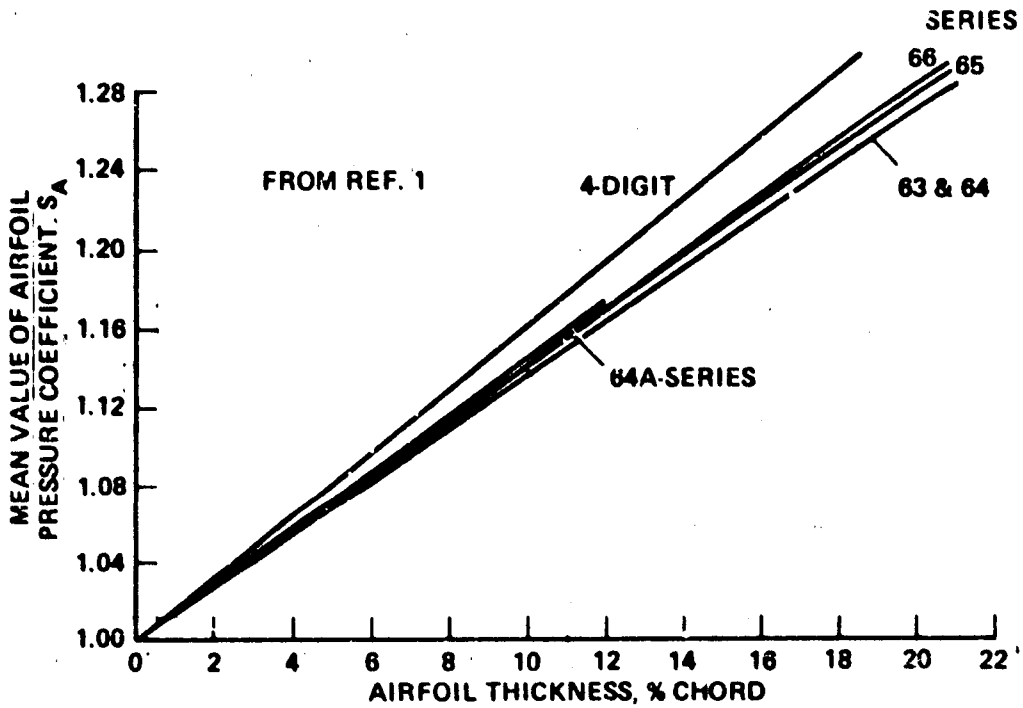

Figure 7.- Airfoil section calculated mean pressure coefficient.

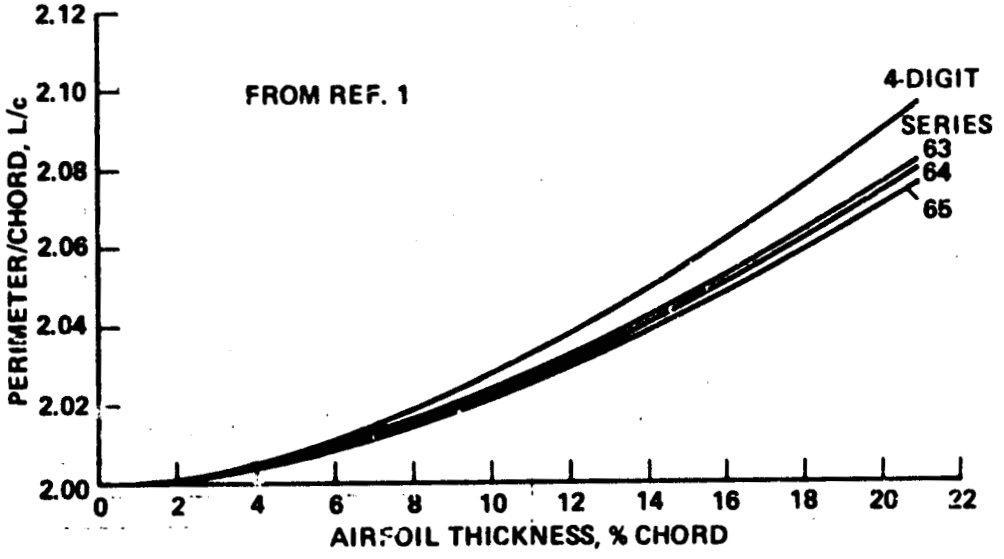

Figure 8.- Airfoil section perimeter/chord ratio.

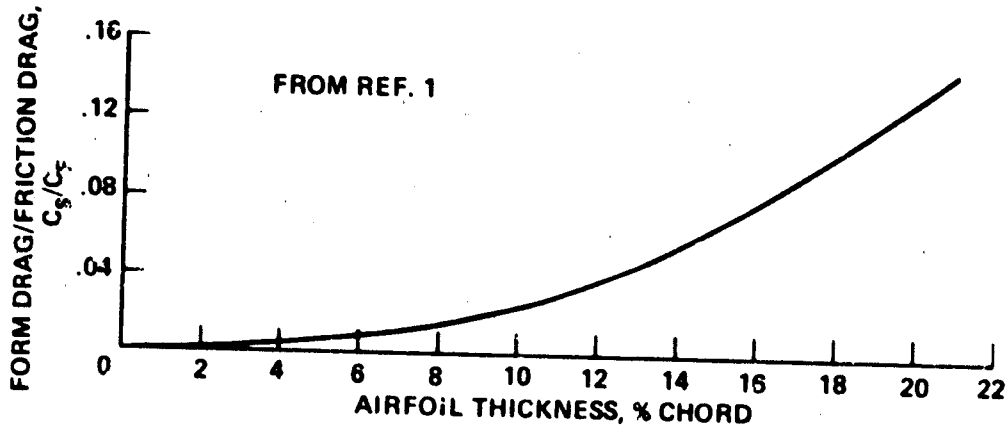

Figure 9.- Airfoil section form drag/friction drag.

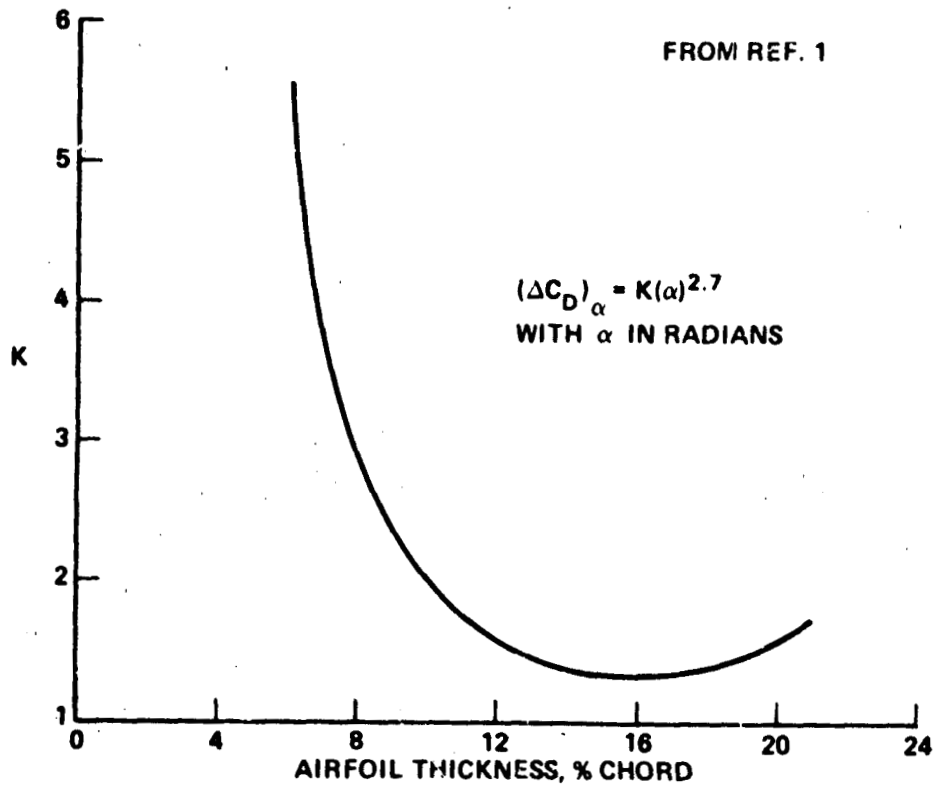

Figure 10.- Correlation parameter for airfoil section drag due to lift.

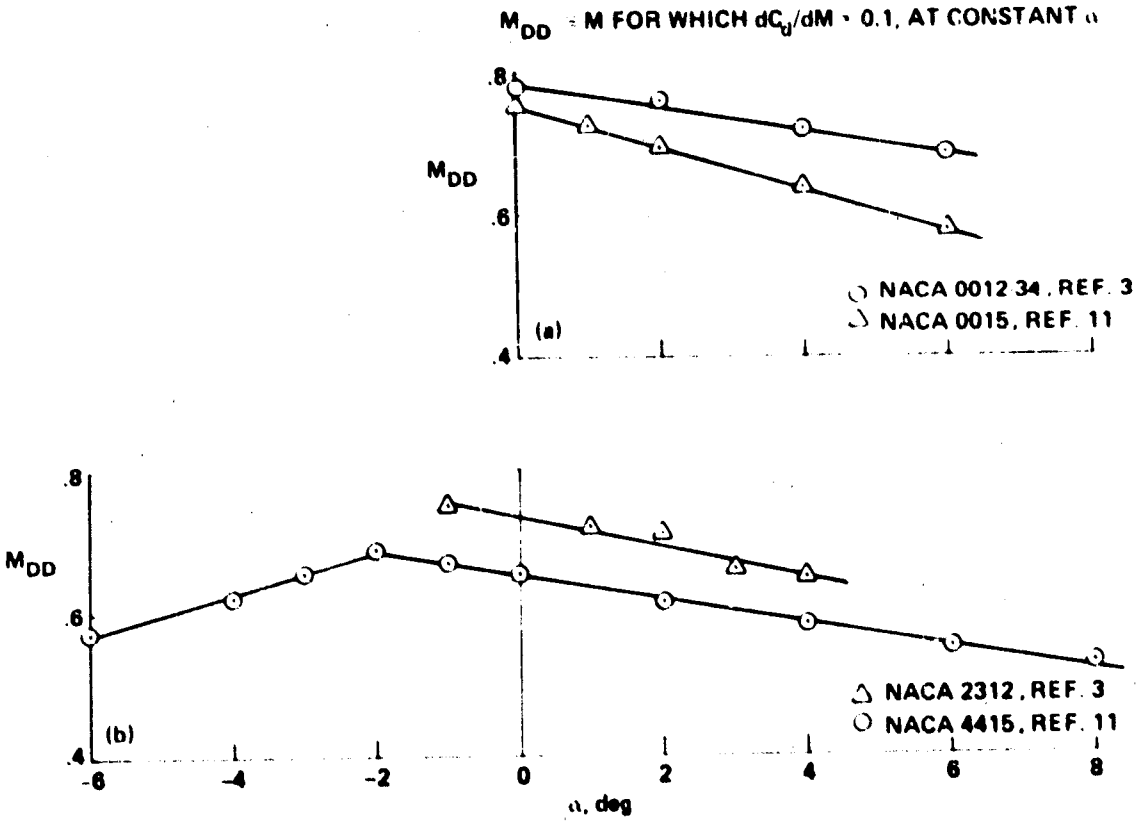

(a) NACA symmetrical four-digit series airfoil sections.

(b) NACA cambered four-digit series airfoil sections.

Figure 11.- Measured airfoil section drag divergence Mach number.

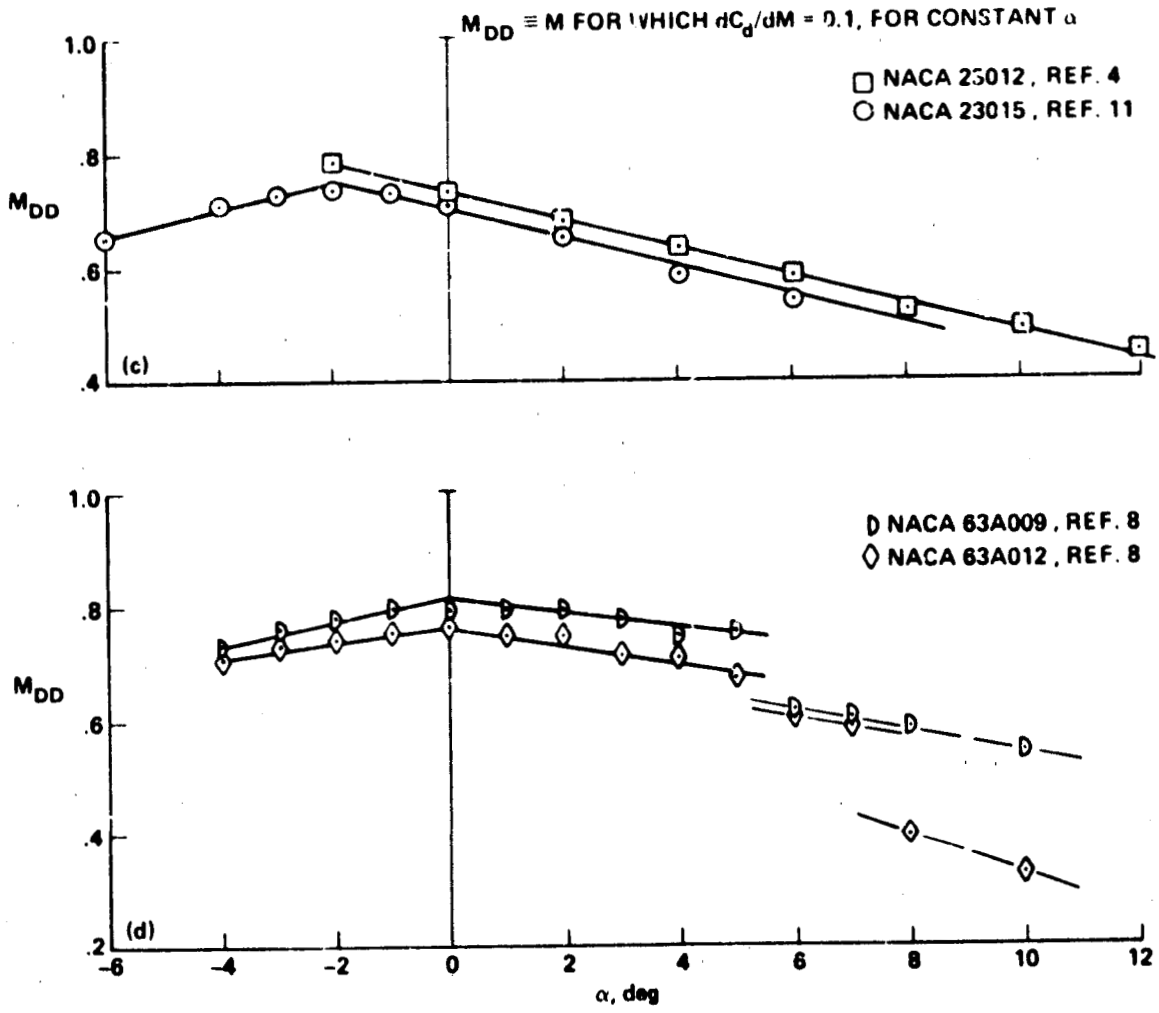

(c) NACA five-digit series airfoil sections.

(d) NACA 63A symmetrical series airfoil sections.

Figure 11.- Continued.

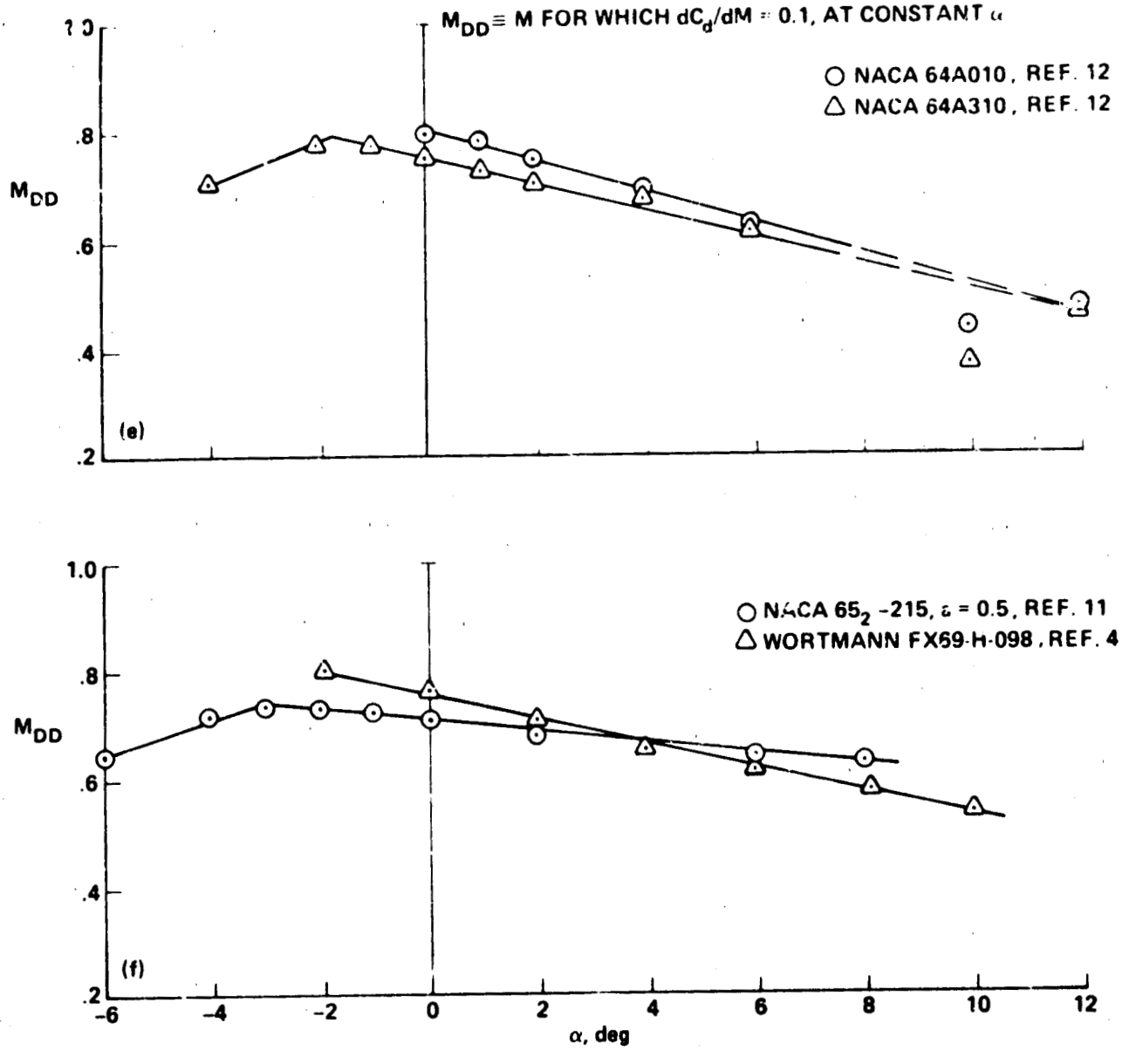

(e) NACA 64A series airfoil sections.

(f) NACA 65 series and Wortmann airfoil sections.

Figure 11.- Concluded.

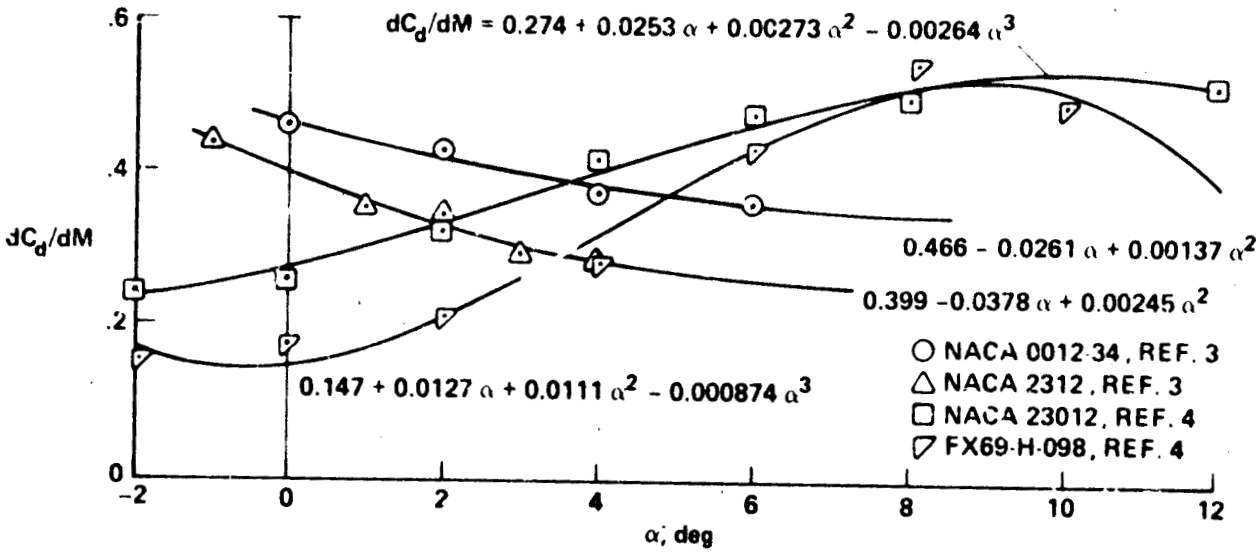

Figure 12.- Slope of c_d curve above drag divergence Mach number.

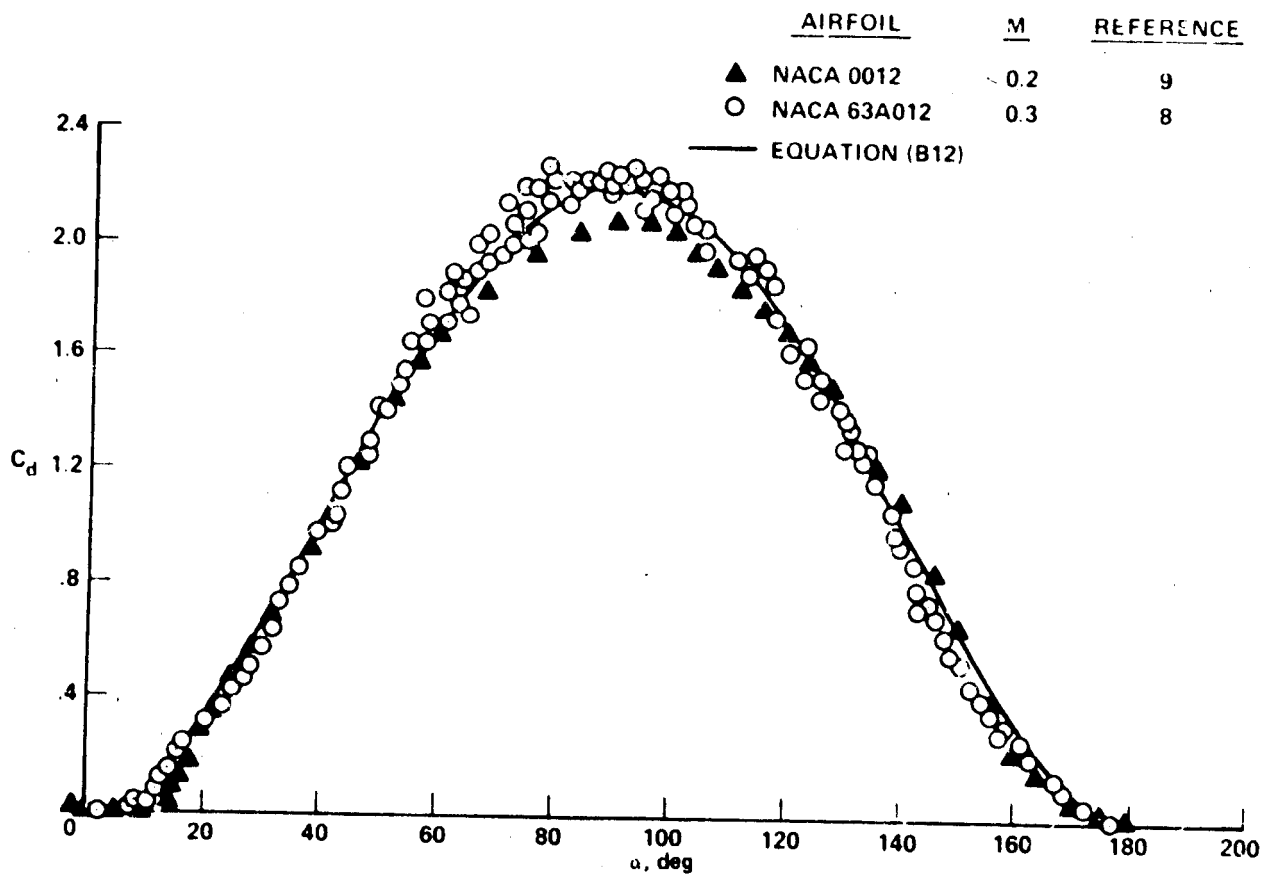

Figure 13.- Airfoil section drag coefficient through 180°.

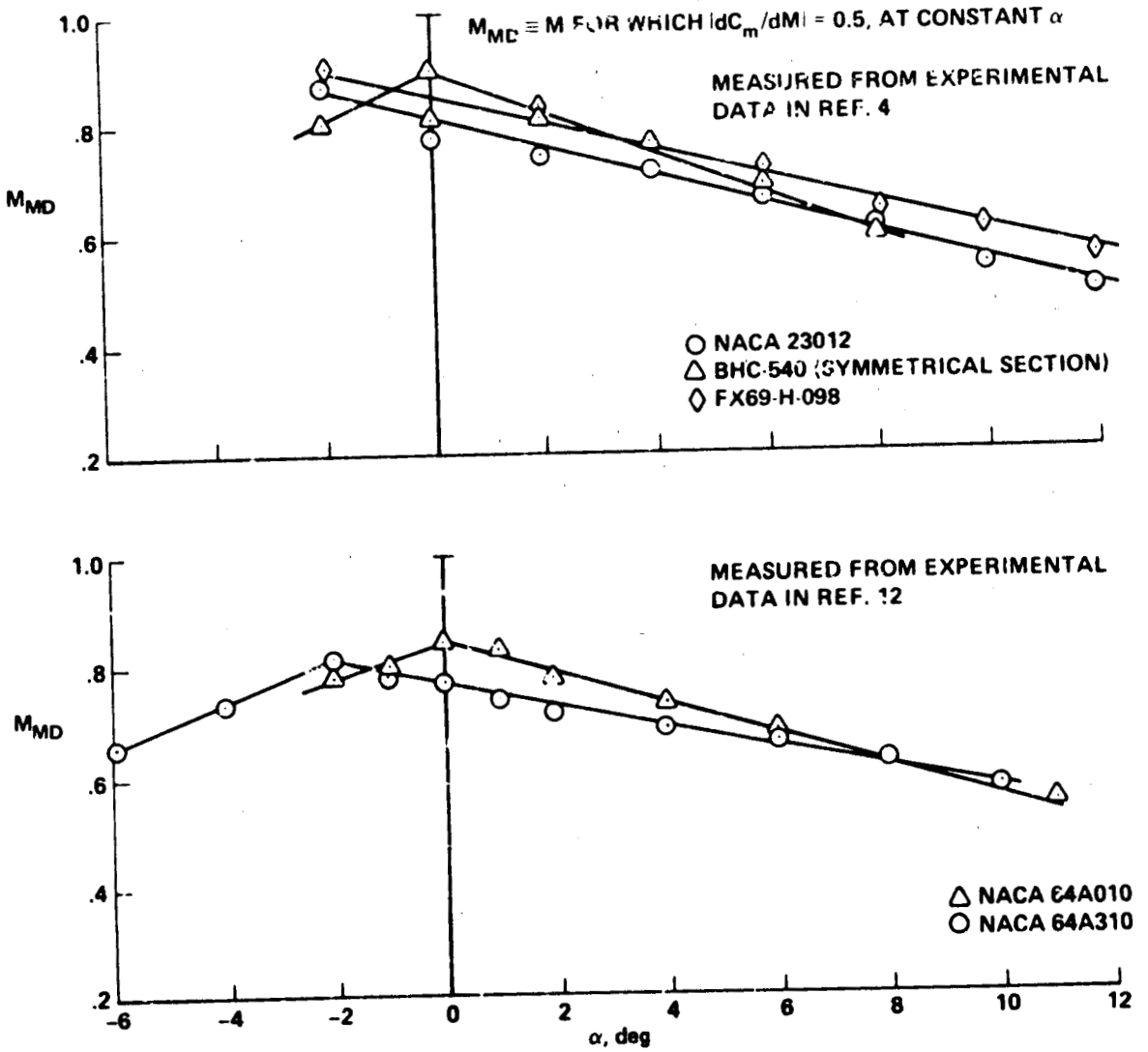

Figure 14.- Measured airfoil section moment divergence Mach number.

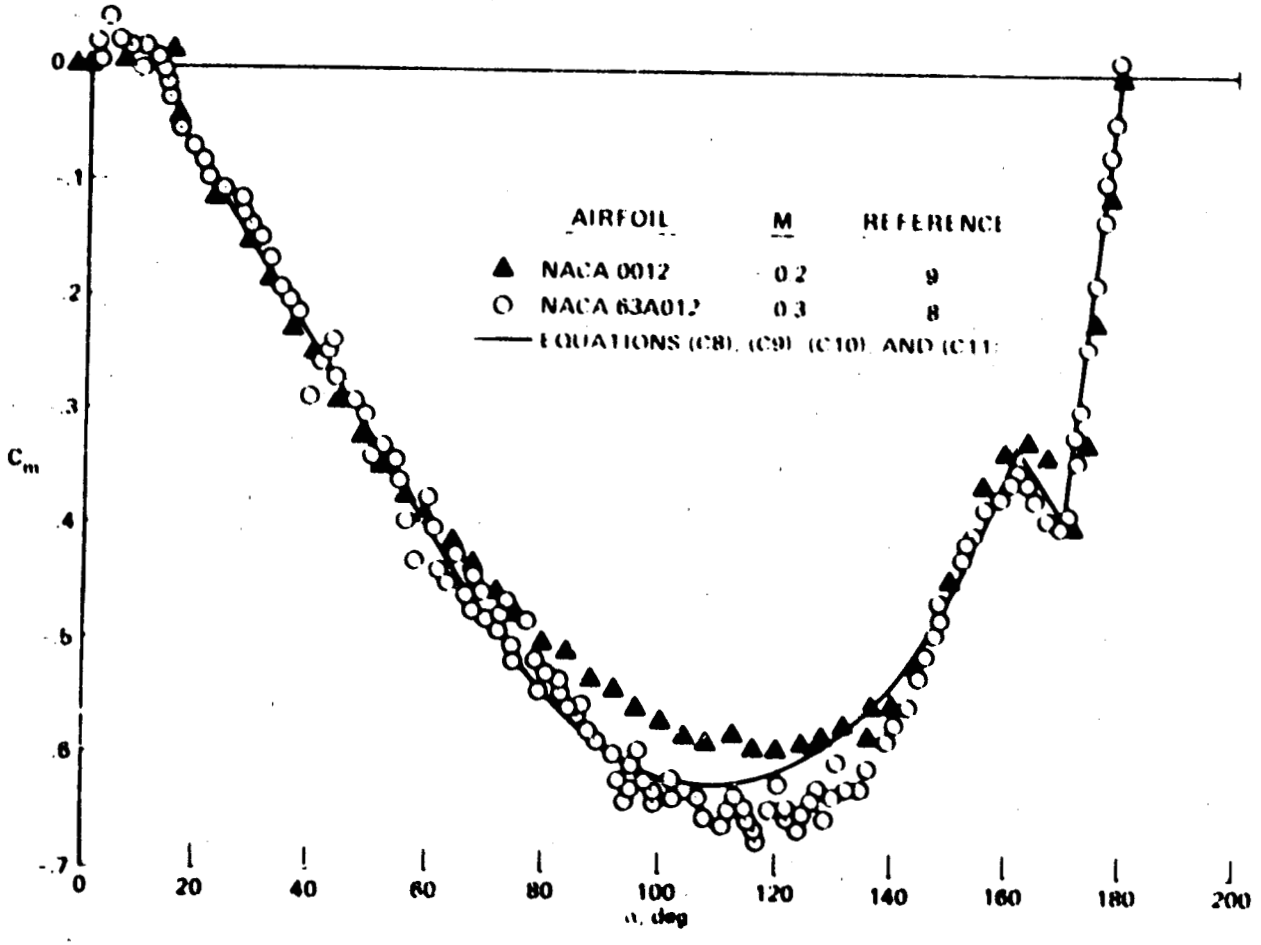

Figure 15. Airfoil section pitching-moment coefficient through 180°.

1 Report No. NASA TM-78492 and AVRADCOM Tech. Rep. 78-15(AM)	2. Government Accession No.	3 Recipient's Catalog No.
4. Title and Subtitle CLOSED-FORM EQUATIONS FOR THE LIFT, DRAG, AND PITCHING-MOMENT COEFFICIENTS OF AIRFOIL SECTIONS IN SUBSONIC FLOW		5 Report Date 6 Performing Organization Code
7 Author(s) Roger L. Smith		8. Performing Organization Report No. A-7466 10 Work Unit No. 992-22-08
9 Performing Organization Name and Address NASA Ames Research Center and Aeromechanics Laboratory, AVRADCOM Research and Technology Laboratories, Ames Research Center Moffett Field, Calif. 94035		11 Contract or Grant No.
12 Sponsoring Agency Name and Address National Aeronautics and Space Administration Washington, D. C. 20546 and Aviation Research and Development Command, St. Louis, Mo. 63166		13 Type of Report and Period Covered Technical Memorandum 14 Sponsoring Agency Code
15 Supplementary Notes		

16 Abstract

Closed-form equations for the lift, drag, and pitching-moment coefficients of two-dimensional airfoil sections in steady subsonic flow are obtained from published theoretical and experimental results. A turbulent boundary layer is assumed to exist on the airfoil surfaces. The effects of section angle of attack, Mach number, Reynolds number, and the specific airfoil type are considered. The equations are applicable through an angle-of-attack range of -18° to +180°; however, above about ±20°, the section characteristics are assumed to be functions only of angle of attack. A computer program is presented which evaluates the equations for a range of Mach numbers and angles of attack. Calculated results for the NACA 23012 airfoil section are compared with experimental data.

17 Key Words (Suggested by Author(s)) Airfoil section characteristics Lift coefficient Drag coefficient Moment coefficient High angle of attack	18 Distribution Statement Unlimited STAR Category - 02		
19 Security Classif. (of this report) Unclassified	20. Security Classif. (of this page) Unclassified	21 No. of Pages 27	22 Price* $4.00

*For sale by the National Technical Information Service, Springfield, Virginia 22161